

## $e^+e^-$ COLLIDING BEAMS PHYSICS

BY L. PAOLUZI

Istituto di Fisica dell'Università — Roma\*  
Istituto Nazionale di Fisica Nucleare, Sezione di Roma

(Presented at the XIV Cracow School of Theoretical Physics, Zakopane, June 15–28, 1974)

The aim of these lectures is to discuss the present experimental situation of  $e^+e^-$  colliding beams physics.

### INTRODUCTION

This field has grown enormously in the past 5 years. In 1969 the total number of papers (both experimental and theoretical) related to such experiments was just a handful, and a very interested physicist could easily bring himself up to date on all developments on  $e^+e^-$  colliding beams physics in an afternoon's reading. Today for someone already immersed in the field it is necessary to launch a major literature search to present a coherent set of timely information, so I have chosen some related topics connected with more recent or, in my opinion, more interesting results.

#### *I. Historical Premise*

The history of  $e^+e^-$  colliding beams begins in 1960 when ADA, an  $e^+e^- 2 \times 220$  MeV colliding beam project, was started in Frascati [1]. After four years of intense and exciting work both at Frascati and Orsay it gave the first measurable luminosity, [2]  $L$ , the central machine parameter defined as the ratio

$$L = \text{rate/cross section} = N/\langle\sigma\rangle$$

for a given reaction.

The  $L$  value was  $10^{25} \text{ cm}^{-2}\text{sec}^{-1}$  a modest and yet significant result demonstrating the technical feasibility of this revolution in accelerators. No unpredictable phenomena was observed with ADA. The luminosity monitoring was committed to a very low momen-

---

\* Address: Istituto di Fisica "G. Marconi", Piazzale delle Scienze, 5 Roma, Italy.

tum transfer Q.E.D. process

$$e\bar{e} \rightarrow e\bar{e}\gamma$$

the single bremsstrahlung at forward angles; even if this process had not yet been observed at these energies the general reliability of Q.E.D. was not in doubt.

Meantime the first modern ring was started at Orsay (ACO, a  $2 \times 500$  MeV colliding beam facility [3]); also news from Siberia about the completion of VEPP-2 [4] ( $e\bar{e} 2 \times 750$  MeV) was collected by visitors at Novosibirsk and participants at the international conferences on high energy particles. Both VEPP-2 and ACO produced the first relevant results for hadron physics by investigating the vector resonances [5]. Their luminosity, about  $3 \times 10^{28} \text{ cm}^{-2}\text{sec}^{-1}$ , was a comfortable value in view of the cross section for vector meson resonances of the order of  $1 \text{ }\mu\text{b}$  at peak.

TABLE I.1

$e^+e^-$  storage rings

Machine	Maximum total c.m. energy GeV	Radius	$L \text{ cm}^{-2}\text{s}^{-1}$	Status
ADA Frascati Italy VEPP-2 Novosibirsk USSR ACO Orsay France ADONE Frascati Italy CEA BY-PASS Cambridge USA SPEAR Stanford USA DORIS Hamburg W.G. DCI Orsay France PETRA SUPERADONE SUPERSPEAR EPIC	 0.5   1.4   1.1   3.0  5.0  5.5 9  7  3.6   $\geq 10$	 0.64   1.6   3.4   16  27  34   46     	 $2 \cdot 10^{25}$   $3 \cdot 10^{28}$ (1 GeV) $3 \cdot 10^{28}$ (1 GeV) $7 \cdot 10^{29}$ (3 GeV) $4 \cdot 10^{28}$ (4 GeV) $6 \cdot 10^{30}$ $10^{32}$ $10^{32}$ $10^{32}$ $10^{32}$	 Active from 1962 to 1965   1966  1967 $\rightarrow$ (1975)  1970 $\rightarrow$  1971 $\rightarrow$ 1973  1973   First injection January 1974  Ready to go on 1975  

A larger ring at  $2 \times 1500$  MeV, ADONE, was completed at the end of 1967. The large circulating currents caused the outset of many new effects in beam dynamics. After various vicissitudes ADONE was ready for physics at the end of 1969 and gave data in the "unknown land" beyond the  $\varphi$  mass. To people content at the time with the simplicity of V.M.D. the copious multihadron production was quite a surprise [6]. This wonder did not yet quench down after the data with the CEA by-pass [7] and SPEAR. The luminosity at ADONE is now at  $10^{30} \text{ cm}^{-2}\text{sec}^{-1}$  level, just surpassed by SPEAR ( $2 \times 2.5$  GeV) with more than  $10^{31} \text{ cm}^{-2}\text{sec}^{-1}$ . The actual situation of colliding beams is reported in Table I.1.

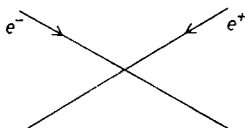
This last year many proposals have been in the air concerning a further generation of storage rings at more than  $2 \times 10$  GeV. The new labels are SUPERADONE, EPIC, PETRA, SUPERSPEAR.

We think that it is due to thrust the construction of at least one high energy facility: the hadrons will perhaps light up by the use of harder rays.

## II. Basic Information About Storage Rings Machine

A typical storage ring machine, ADONE, is shown schematically in Fig. 1. The beams, injected at low energy from the deflecting channels, are accelerated into two R.F. cavities and cross each other in 6 interactions regions, 4 of which can be used for experiments (R.F. cavity in the others).

In the project an angle collision



was foreseen, but the machine has functioned only with head-on collision, which gave some trouble to the already built experimental set-ups, because it made the interaction region longer.

There are 3 bunches per beam, so that the distance in time between bunches is of the order of 100 nsec, and the luminosity lifetime, with injected currents of the order of 50 mA at 1 GeV beam energy, is in the 5–10 hours range.

Total luminosity is  $\sim 10^{30} \text{ cm}^{-2}\text{sec}^{-1}$  from 2.0 to 3.0 GeV total energy and decreases strongly below 2 GeV with energy ( $L = 5 \times 10^{28}$  at  $2E = 1.2$  GeV). The beam size and energy spread are given by r.m.s. width of target densities ( $E$  in GeV)

$$\sigma_{\text{transv.}} = 0.1 E \text{ cm}, \quad \sigma_{\text{long.}} = 20 E^{3/2} \text{ cm}, \quad \sigma_{\text{energy}} = E^2 \text{ MeV}.$$

We use the following equivalent notations

$$W = 2E = \sqrt{s} = \sqrt{q^2}$$

for the total energy of the  $e\bar{e}$  system.

Luminosity can be measured via small momentum transfer reactions, as

- (1)  $e\bar{e} \rightarrow e\bar{e}$  Bhabha and Møller scattering,
- (2)  $e\bar{e} \rightarrow e\bar{e}\gamma$  simple bremsstrahlung (S.B.),
- (3)  $e\bar{e} \rightarrow e\bar{e}\gamma\gamma$  double bremsstrahlung (D.B.),
- (4)  $e\bar{e} \rightarrow \gamma\gamma$  annihilation.

All these processes are peaked forward but not to the same extent (the order 1  $\rightarrow$  4 is the one of lesser peaking). In principle any of these processes can be used as a monitoring reaction. Yet since the reaction (4) has a small cross section compared to (3), the separation

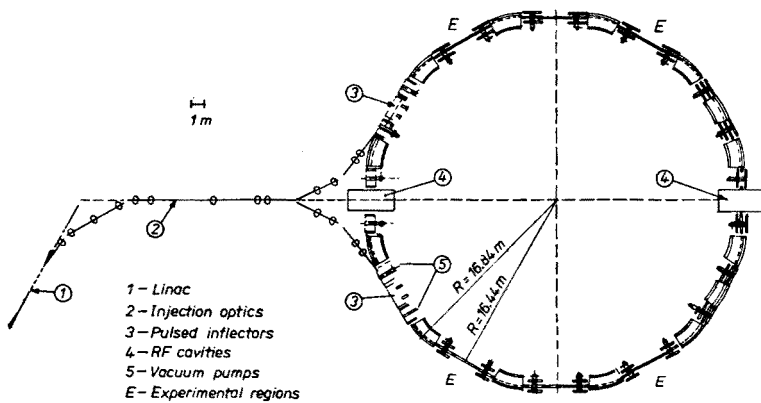


Fig. 1. Storage ring lay-out (ADONE)

of the monochromatic  $\gamma$  rays of (4) from the continuum of (3) is not easy. Reaction (3) is a good monitoring reaction as long as chance coincidences from (2) are not too high. This limits D.B. use at values for luminosity less than a few  $10^{30} \text{ cm}^{-2} \text{ sec}^{-1}$ . S.B. leads to a very high counting rate with dead time problems for  $L \sim 10^{31}$ ; reaction (1) can be used in a wide range of  $L$ . Its main draw-back is that it requires a very precise geometrical arrangement to achieve an absolute monitor.

Now currently wide angle Bhabha scattering in the main experimental apparatus is used as a monitor, this procedure being perhaps free of some systematic errors.

Electron polarization [8] can present a big problem if, as in the ADONE case, the experimental set-ups do not cover all the  $\varphi$  angles. For example  $e^+e^- \rightarrow \mu^+\mu^-$  distribution is given by

$$\sigma_{\text{POL.BEAMS}}(e^+e^- \rightarrow \mu^+\mu^-) = \sigma_{\text{WITHOUT POL.}} \left[ 1 + |P_+| |P_-| \frac{\beta_\mu^2}{2 - \beta_\mu^2 \sin^2 \theta} \cos 2\varphi \right],$$

where  $\varphi$  is the angle between the plane of the beam orbit and the plane of the reaction.

Electron spin polarization has not been measured on ADONE; its rise time is predicted to be

$$\tau = \frac{11.5}{E^2} \text{ hours,}$$

if depolarizing effects are not present. Recent analysis on  $\mu^+\mu^-$  distributions do not show any polarization effect.

### III. Physics

I am dividing the topics I will talk about into the following:

1. First order Q.E.D. high momentum transfer processes
2. Two photons processes ( $\gamma\gamma$  collisions)
  - a) producing lepton pairs
  - b) producing hadrons
3. Collinear hadrons production (study of e.m. form factor of hadrons)
4. Multihadron, via one photon, production.

#### 1. First order Q.E.D. high momentum processes

The three classical reactions for the study of the validity of Q.E.D. with  $e^+e^-$  colliding beams are

$$(1) \quad e^+e^- \rightarrow e^+e^-,$$

$$(2) \quad e^+e^- \rightarrow \mu^+\mu^-,$$

$$(3) \quad e^+e^- \rightarrow \gamma\gamma.$$

I will not discuss results of  $\gamma\gamma$  production as I do not know the new recent results on this subject. This channel was studied at Novosibirsk [9], Frascati [10] and CEA [11] with spark chamber technique, and more recently with Na I counters technique at SPEAR [12]. No significant deviations from Q.E.D. were found.

The Q.E.D. calculations for processes (1) and (2) are based on the assumptions that:

- (1) Leptons behave like point-like Dirac particles;
- (2) Maxwell equations are valid; the photon propagator is simply given by  $1/q^2$ ;
- (3) One photon diagrams dominate in the calculation and contributions from higher order diagrams can be taken care of by the usual method of radiative corrections.

The validity of these assumptions has been tested with increasing accuracy and over increasingly large energy regions. So I will discuss only the results at higher energy, which are recent preliminary data from the SPEAR magnet experiment [13].

The set up is shown in Fig. 2 and consists of a succession of cylindrical shells, immersed into a magnetic field, each one being a detector which accomplishes a particular detection function (Wire Proportional Chambers to measure convergence, Magnetostrictive Spark

Chambers to measure particles momentum, scintillation counters to measure height pulse amplitude...).

The experimental separation of  $ee$  and  $\mu\mu$  channels is shown in Fig. 3 where the events are selected by the request of two particles collinearity, timing with the collision time, and convergence in the interaction region.

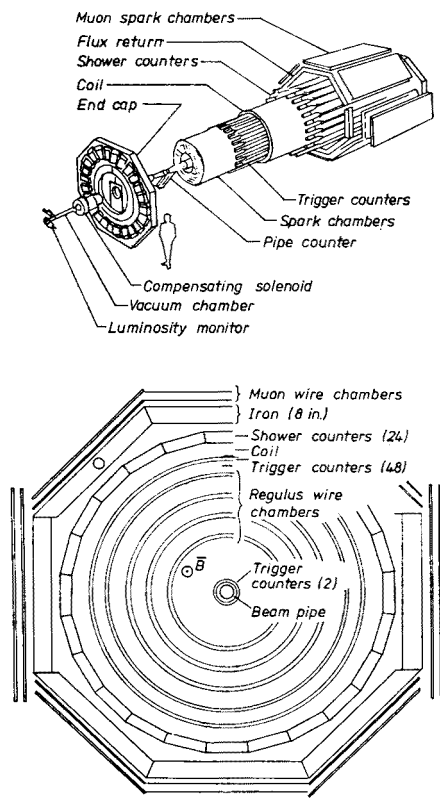


Fig. 2. SPEAR magnet set-up

The results are shown in Figs 4, 5, 6 where a very good agreement with Q.E.D. predictions is seen.

It has been customary to parametrize a possible violation by means of a parameter  $\Lambda$ , which has the dimensions of a momentum transfer, which is introduced in a possible modification of the virtual photon propagator according to

$$\frac{1}{q^2} \rightarrow \frac{1}{q^2} - \frac{1}{q^2 - \Lambda^2} = \frac{1}{q^2} \frac{1}{1 - q^2/\Lambda^2}, \tag{1}$$

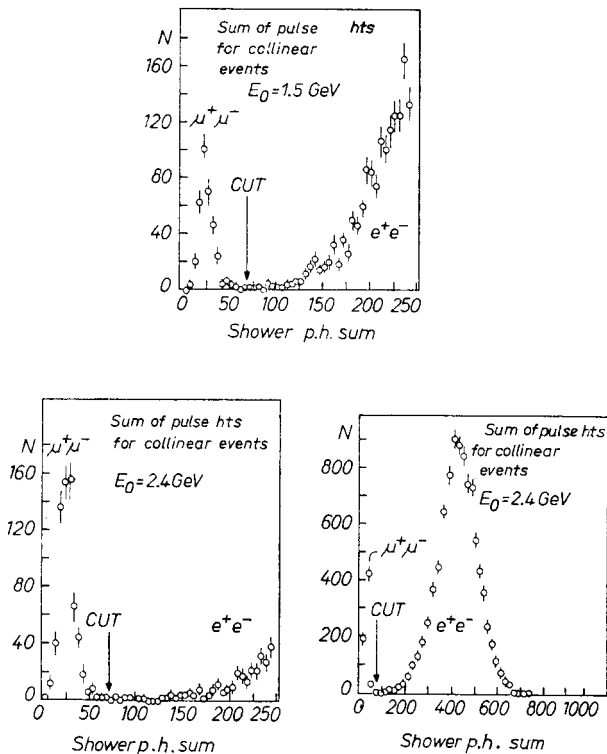


Fig. 3.  $\mu\bar{\mu}$  and  $e\bar{e}$  separation from pulse height determination in the shower counters (SPEAR, preliminary data)

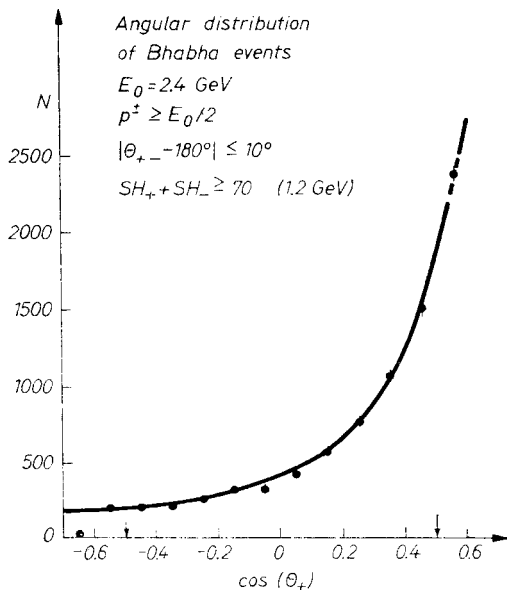


Fig. 4. Angular distribution of Bhabha events (preliminary data)

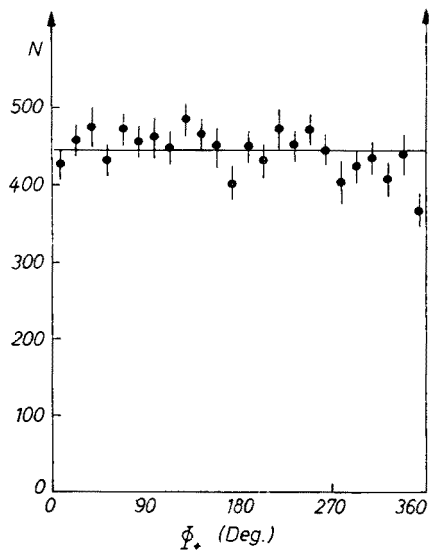


Fig. 5. Azimuthal distribution of Bhabha events (preliminary data)

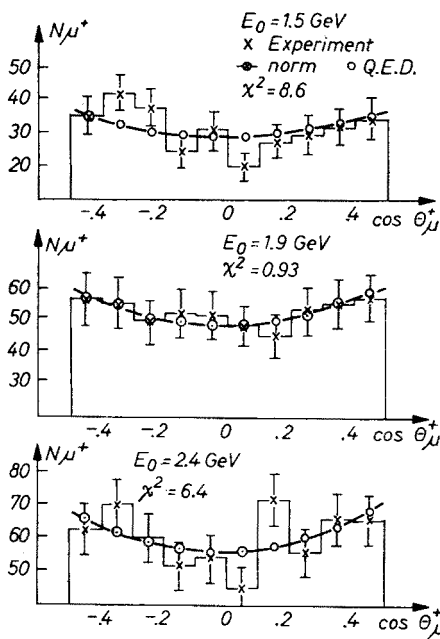


Fig. 6. Angular distribution of  $\mu^+\mu^-$  events (preliminary data)



such an alteration can be interpreted as a modification of Coulomb potential

$$\frac{1}{r} \rightarrow \frac{1}{r} (1 - e^{-\Lambda r/\hbar}). \tag{2}$$

Because of the minus sign in front of the added term in (1), such a modification violates the general spectral representation of the photon propagator established by Källén and Lehmann, which is based on local relativistic fields.

Since one is looking for some deviations from Q.E.D. one might wonder which are the fundamental principles one wants to stick to, and which should be abandoned. Obviously there is room for many models which look for alteration of theory. These remarks explain why the experimentalists often try both a modification like (1) and a modification of the form

$$\frac{1}{q^2} \rightarrow \frac{1}{q^2} + \frac{1}{q^2 - \Lambda^2}. \tag{3}$$

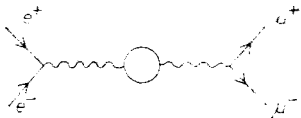
In the Table III.1.1 I have summarized the results on  $\Lambda_{\pm}$  from the various storage rings. With comparable systematic errors, due to monitoring, it is clear that higher energy results give higher  $\Lambda_{\pm}$  cuts including the previous lower energy results.

TABLE III.1.1

	STANF $e^-e^-$ $2 \times 556$	ORSAY $2 \times 210$ $e^+e^-$	ADONE $2 \times 900$ $e^+e^-$	ADONE $2 \times 900$	SPEAR $2 \times 2000$ $e^+e^-$ (Preliminary)	SPEAR $2 \times 2400$ $e^+e^-$ (Preliminary)
$\Lambda_+^T$ (GeV)	2.7	—	—	—	8.6	24
$\Lambda_-^T$ (GeV)	4.0	—	—	—	11.0	20
$\Lambda_+^S$ (GeV)	4.4	—	—	—	12.0	—
$\Lambda_-^S$ (GeV)	2.5	—	—	—	10.0	—
$\Lambda_S = \Lambda_T)^+$ (GeV)	—	2.1	—	—	19	—
$(\Lambda_S = \Lambda_T)^-$ (GeV)	—	3.6	6.0	10.0	24	—

Before leaving the one photon lepton pair processes I want to talk about two more results.

The first is a very interesting measure by a group at ACO [14]. By making accurate measurements of the  $s$  dependence of  $e^+e^- \rightarrow \mu^+\mu^-$  near the  $\varphi$  mass they observed the contribution to vacuum polarization due to the  $\varphi$  intermediate state via the diagram



A total of 2300  $\mu^+\mu^-$  pairs were observed. The results of the analysis of this experiment are shown in Fig. 7 and give evidence for hadronic polarization with a confidence level higher

than 95%

$$\Gamma_{\varphi \rightarrow e^+e^-} / \Gamma_{\varphi \rightarrow \text{all}} = (2.6 \pm 1.0) \times 10^{-4}.$$

The second result concerns the direct search for possible heavy leptons.

The clearest way to look for these leptons in  $e^+e^-$  experiments is to look for their possible decay modes in which  $\mu$ 's and electrons are involved. In fact, hadronic channels

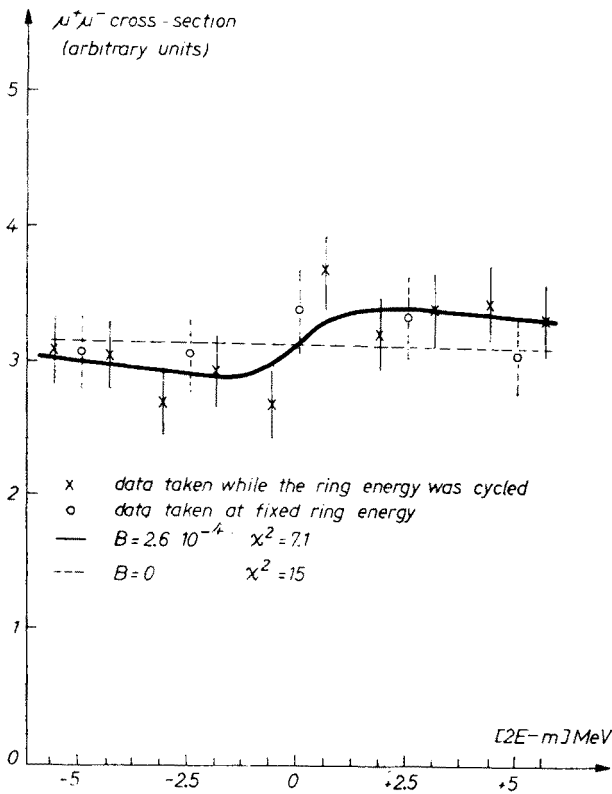
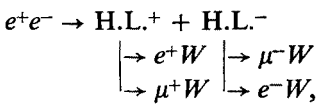


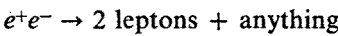
Fig. 7. Experimental results obtained with ACO on the  $\mu\bar{\mu}$  yield at energies close to the  $\varphi$  meson mass

could be heavily contaminated by other competing reactions. Both BCF [15] and  $\mu\pi$  [16] groups at ADONE searched for mixed leptonic modes



where non-collinear and non-coplanar (with respect to the beam axis)  $e$ -like and  $\mu$ -like tracks in spark chambers should appear.

Furthermore the energy dependence of the reactions



was inspected looking for anomalous threshold-like effects since the production cross section as a function of energy is expected to show peculiar patterns when the available energy is such as to produce a heavy lepton.

No events of the type  $e-\mu$  were found. In order to put a limit to the production rate of possibly heavy leptons, the decay rate for the leptonic and hadronic modes, and the parameters for leptonic decay must be estimated.

For three reasonable types of heavy leptons,  $E$ ,  $M$ ,  $H$  respectively with the same leptonic number as electrons, the same leptonic number as muons, and a new leptonic number an upper limit at 1.15 GeV at a 95% confidence level was given.

It can be remembered that by neutrino experiments at CERN and NAL new mass limits for the heavy lepton  $M$  at 2.4 GeV and 2.0 GeV were reported. The  $e^+e^-$  ADONE limit of 1.15 GeV is still relevant, however, for the heavy leptons  $E$  and  $H$  as defined above. I have not noticed, up to now, a similar search by SPEAR.

## 2. Two-photon interaction processes

The electron-positron storage rings made available, besides the one-photon exchange reaction realm, also the appealing world of the two-photon collision processes. In these processes, two virtual photons are exchanged in the lowest order and  $C = +1$  states are produced (either leptonic or hadronic) according to the well known diagrams shown in Fig. 8.

In spite of the fact that the cross section for two photon exchange processes is depressed by a factor  $\alpha^2$  with respect to the usual one photon annihilation graphs, due to the higher probability that low-energy virtual photons have to be emitted, the cross section for the two-photon processes increases logarithmically with energy and rather soon becomes com-

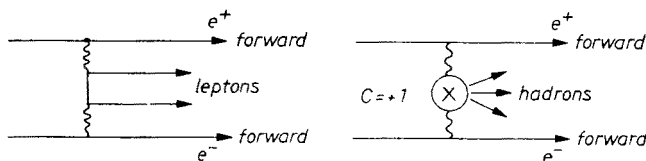


Fig. 8.  $\gamma\gamma$  processes diagrams

parable with the one-photon annihilation cross section. By following the Weizsäcker-Williams approximation, the incoming electron and positron are replaced by their equivalent radiation fields whose content may be represented according to the following expression for  $p(k)dk$ , the probability for an electron (or positron) of a given energy  $\sqrt{s}$  to bring a photon whose energy is in the range  $k-k+dk$ ,

$$p(k)dk = \frac{2\pi}{\alpha} \frac{dk}{k} L\left(\frac{2k}{\sqrt{s}}, s\right),$$

where

$$L(x, s) = \frac{1}{4} [1 + (1-x)^2] \ln \frac{s}{4m_e^2}.$$

Then, by assuming that the process

$$e^+e^- \rightarrow e^+e^-X$$

(1)

is due to the interaction of two photons which produces the final state  $X$  with total cross section  $\sigma_{\gamma\gamma\rightarrow X}(\bar{s})$ ,  $\bar{s}$  being the square of the total energy of the  $\gamma\gamma$  system in their c.m.s., the cross section for the process (1) is given by:

$$\sigma(e^+e^- \rightarrow e^+e^-X) = \frac{1}{2} \left( \frac{\alpha}{\pi} \ln \frac{s}{4m_e^2} \right)^2 \int_{s_t}^s \frac{d\bar{s}}{\bar{s}} f\left(\frac{\bar{s}}{s}\right) \sigma_{\gamma\gamma\rightarrow X}(\bar{s}),$$

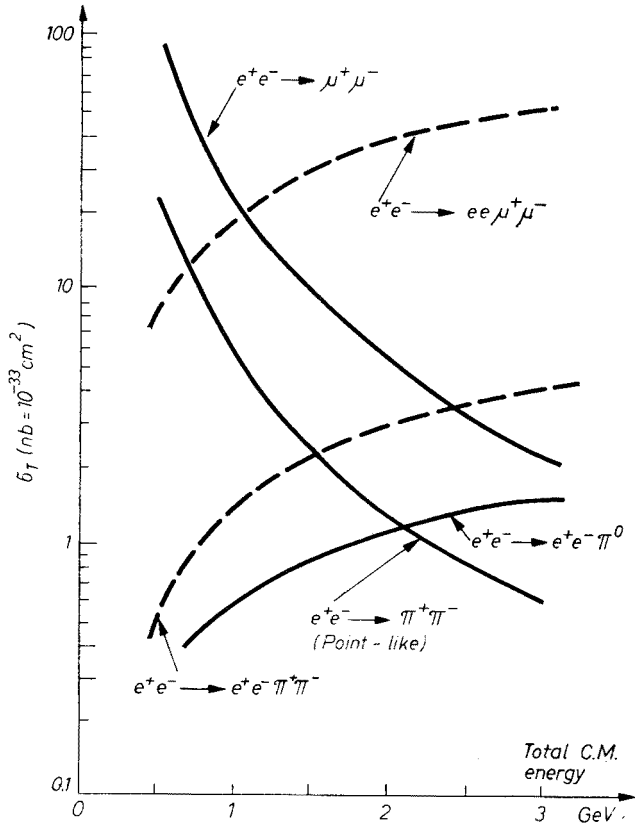


Fig. 9.  $\gamma\gamma$  processes total cross sections

where  $f(y) = \frac{1}{2}(2+y)^2 \ln 1/y - (1-y)(3+y)$  and  $s_t$  is the threshold energy for the process  $\gamma\gamma \rightarrow X$ . In Fig. 9 a comparison between some one-photon and two-photon reaction cross section is shown. It is worth noticing that the two-photon cross sections rather soon become comparable with the one-photon cross sections: in the case of muon pair production, for instance,  $\sigma(ee \rightarrow ee\mu\mu) \simeq (ee \rightarrow \mu\mu)$  at about 1 GeV energy. The experimental discrimination between the two reactions is however clean and, at least at the ADONE energies, reciprocal contamination problems may be safely ruled out.

In this respect the photon-photon processes exhibit a series of experimental peculiarities which make them rather easily detectable (at least in ADONE) and give them clean signatures. The most relevant of these properties are the following: both the incoming electron and positron radiate a photon, and are emitted forward bringing only a fraction of the primary energy, so that they can be detected by a suitable tagging systems [18–21] which also measure their final energies; the photon-photon invariant mass  $M_{\gamma\gamma}$  is therefore known together with the velocity of the center of the mass of the  $\gamma\gamma$  system; in the case of two-body production, the knowledge that the line of flight of the center of mass of the  $\gamma\gamma$  system lies within a known spread around the beam line allows very selective coplanarity constraints and, when the energy of the wide angle emitted particles is known, also transverse momentum balance requirements.

By properly making use of the mentioned experimental characteristics the two-lepton production has been studied in Novosibirsk [22] and Frascati [18, 20, 21, 23, 24] while the two-photon annihilation into pion pair and many hadrons have been also detected in Frascati [25, 26].

As far as the photon-photon two-lepton production is concerned, both the reactions

$$e^+e^- \rightarrow e^+e^-e^+e^-, \quad (2)$$

$$e^+e^- \rightarrow e^+e^-\mu^+\mu^-, \quad (3)$$

have been detected in several kinematical configurations.

In the first Novosibirsk experiment [22] only wide angle coplanar (coplanarity angle less than  $10^\circ$ )  $e^+e^-$  pair events were looked for. The experimental acoplanarity angle distribution for the detected events was compared with the Q. E. D. predictions for the process and a satisfactory agreement found.

The ADONE experiments [20, 21, 23–26] were equipped with tagging systems installed inside the bending magnets of ADONE adjacent to the experimental straight sections. The machine bending magnets acted as momentum analysers for the forward emitted electron and positrons if the processes (1). The main properties of the tagging system are shown in Table III. 2.1.

TABLE III.2.1

ADONE tagging systems [19].  $P$  indicates the forward emitted  $e^\pm$  momentum and  $E$  is the single beam momentum

Momentum acceptance	$0.1 \leq p/E \leq 0.9$
Momentum resolution	$\frac{\Delta p}{p} = \pm 4\% \quad \text{at} \quad \frac{p}{E} = 0.7$
Angular acceptance	$\Delta\theta_{\text{vert}} = \pm 8 \text{ mrad}$
Geometrical efficiency	$\sim 50\%$

A sketch of one experimental set-up active in ADONE in the period 1971–72 is shown in Fig. 10. The relevant kinematical quantities directly measurable with these apparata are shown in Fig. 12, where 1 and 2 label the wide angle emitted particles coplanar with the

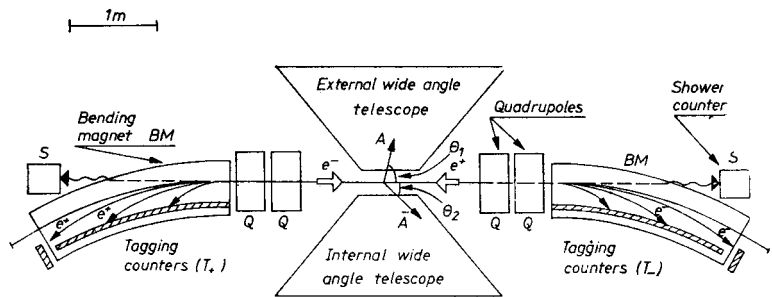


Fig. 10. Sketch of the set-up for the tagging system

beams when produced by the interaction of two photons of energy  $k_+$  and  $k_-$ , respectively. The center of mass of the wide angle emitted particles 1 and 2 moves along the beam direction with a velocity

$$\beta = \frac{k^+ - k^-}{k^+ + k^-} = \frac{\sin (\theta_1 + \theta_2)}{\sin \theta_1 + \sin \theta_2}.$$

TABLE III.2.2

The reaction  $e^+e^- \rightarrow e^+e^-e^+e^-$  as studied at ADONE: events in various final state detected configurations and results of the analyses. Average total energy 2.7 GeV

Detected particles		Measured quantities	Events + luminosity	Analysis	Ref.									
Wide angle forward														
$e^+, e^-$	$e^\pm$	$\theta_1, \theta_2$	44 in $168 \text{ nb}^{-1}$	$\beta(\theta_1, \theta_2)$ distribution compared with E.P.A. predictions virtual photon contribution evidenced (see Fig. 11)	[20] [23]									
$e^+, e^-$	$e^+, e^-$	$\theta_1, \theta_2$ $k_+, k_-$	12 in $290 \text{ nb}^{-1}$	Check of the relationship $\beta(\theta_1, \theta_2) = \beta(k_+, k_-)$ . Comparison with the E.P.A. predictions on the absolute rate satisfactory: expected number of events $(11.6 \pm 1.1)$	[21]									
$e^+, e^-$	$e^\pm$	$\theta_1, \theta_2$ $k_\pm$	64 in $290 \text{ nb}^{-1}$	On the basis of the calculated energy of the photon possibly associated with the undetected forward $e^\pm$ a separation is made between events $\gamma\gamma \rightarrow e^+e^-$ with quasi real photons (Q.R.P.) and events from deeply virtual photon contribution (V.P.): <table><tr><th>Type</th><th>Observed</th><th>EPA expected</th></tr><tr><td>Q.R.P.</td><td><math>49 \pm (6) \pm 7</math></td><td><math>41 \pm 5</math></td></tr><tr><td>V.P.</td><td><math>15 \pm (6) \pm 4</math></td><td><math>18 \pm 9</math></td></tr></table>	Type	Observed	EPA expected	Q.R.P.	$49 \pm (6) \pm 7$	$41 \pm 5$	V.P.	$15 \pm (6) \pm 4$	$18 \pm 9$	[21]
Type	Observed	EPA expected												
Q.R.P.	$49 \pm (6) \pm 7$	$41 \pm 5$												
V.P.	$15 \pm (6) \pm 4$	$18 \pm 9$												

The c. m. velocity  $\beta$  can be therefore determined either by measuring  $k_+$  and  $k_-$  when both the forward emitted electron and positron are detected by the tagging system and their energies measured, or by measuring the wide angle particle emission angles  $\theta_1$  and  $\theta_2$ . When all the four quantities are simultaneously measured a check of the above

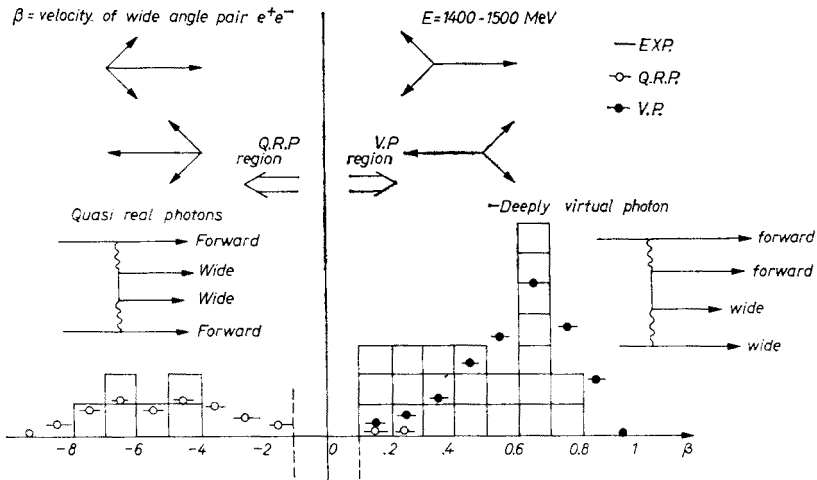


Fig. 11. Experimental results from  $\gamma\gamma$ -group (ADONE) on  $e\bar{e} \rightarrow e\bar{e}e\bar{e}$

mentioned relationship  $\beta(k_+, k_-) = \beta(\theta_1, \theta_2)$  is also made. The experimental  $\beta$  distribution in a given sample of two-lepton photon-photon produced event as well as the absolute rates are also compared with the equivalent photon approximation prediction (E.P.A.). A summary of the experimental situation and the results of the analyses performed in the

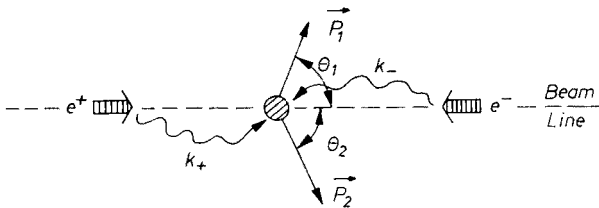


Fig. 12. Kinematics of two body  $\gamma\gamma$ -production

$e^+e^- \rightarrow e^+e^-e^+e^-$  channel is shown in Table III.2.2. It is worth recalling that in analysing the  $e^+e^+ \rightarrow e^-e^-e^+e^-$  events the contribution of deeply virtual photon processes has been clearly evidenced with respect to the "quasi real" interactions shown in Fig. 8: that is the mechanism according to which a primary  $e^\pm$  irradiates a photon which converts into a forward emitted pair, one member of which undergoes an elastic scattering with the other primary  $e^\pm$ . The main experimental feature of this contribution is, besides

the peculiar distribution (see Fig. 11), the kinematical configuration which occurs with both the forward emitted particles in the same tagging region. In principle [27], this mechanism could be used in order to investigate  $e\text{-}\mu$ ,  $e\text{-}\pi$ ,  $e\text{-}k$  scattering as shown in Fig. 13.

As far as the  $e^+e^- \rightarrow e^+e^-\mu^+\mu^-$  reaction is concerned, the situation is sketched in Table III.2.3. The identification of the  $\gamma\gamma \rightarrow \mu^+\mu^-$  events [21] was based on the muon-like

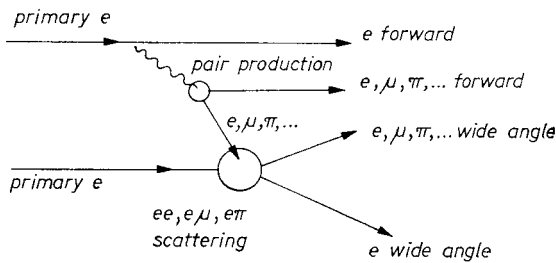


Fig. 13. Diagram for “deeply virtual” photon processes

behaviour of the wide angle emitted particles in the materials of the telescopes and, one their muonic nature was tested, on the kinematical constraints connecting the measured quantities. In practice, knowing  $\theta_1, \theta_2$  and  $p_{1,2}$  it is possible to reconstruct the value of the photon energies  $k_+^{\text{rec.}}$  and  $k_-^{\text{rec.}}$ , and compare them with the tagging measured values  $k_+^{\text{meas.}}$  and  $k_-^{\text{meas.}}$ . The result of this comparison is shown in Fig. 14 where the  $k = (k^{\text{rec.}} - -k^{\text{meas.}})$  distribution is plotted for the 10 double-tagging  $\mu$ -events.

It has been already mentioned that in addition to the lepton pair production, the photon-photon processes may provide a powerful tool for investigating  $C = +1$  meson resonances which couple to the  $\gamma\gamma$  state (such as  $\varepsilon, \eta, \eta', \dots$ ). Following these lines a first

TABLE III.2.3

A summary of the results obtained at ADONE [5] on the reaction  $e^+e^- \rightarrow e^+e^-\mu^+\mu^-$  at an average total energy of 2.7 GeV

Detected wide angle	Particles forward	Measured quantities	Events + luminosity	Analysis
$\mu^+, \mu^-$	$e^+, e^-$	$\theta_1, \theta_2$  $k_+, k_-$ , at least one $\mu$ -momentum $p_{1,2}$ (range)	10 in $290 \text{ nb}^{-1}$	$\Delta k = (k^{\text{rec.}} - k^{\text{meas.}})$ distribution correctly peaked around zero. E.P.A. expected number of events = $11 \pm 1$ , which compares with 10 experimental events. Also photon momentum distribution agrees with E.P.A.
$\mu^+, \mu^-$	$e^\pm$	$\theta_1, \theta_2$ ,  $k_\pm, p_1$ , $p_2$	20 in $290 \text{ nb}^{-1}$	E.P.A. expected number of events = $28 \pm 2.6$



experimental study has been performed in Frascati, [25, 26], on the processes  $\gamma\gamma \rightarrow \pi^+\pi^-$  and  $\gamma\gamma \rightarrow$  many hadrons via the reactions:

$$e^+e^- \rightarrow e^+e^-\pi^+\pi^-, \quad (4)$$

$$e^+e^- \rightarrow e^+e^- + \text{multihadrons.}$$

Even if within a limited statistics, evidence has been found for the processes (4) and (5). A summary of the relevant experimental requirements and the collected data is shown in Table III.2.4.

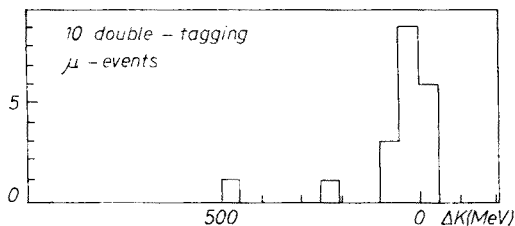


Fig. 14.  $\Delta k = (k^{\text{meas.}} - k^{\text{rec.}})$  distribution for double-tagged events

In order to interpret the data for reactions such as  $\gamma\gamma \rightarrow$  hadrons, it may be useful to recall that when, (neglecting the Born term contribution [11]) a resonant channel opens via the mechanism  $\gamma\gamma \rightarrow R \rightarrow$  hadrons ( $R$  being a resonance of mass  $M$  and spin  $J$ ), then the cross section for the process  $e^+e^- \rightarrow e^+e^-R$  is directly connected to the  $R \rightarrow \gamma\gamma$  width,  $\Gamma_{R \rightarrow \gamma\gamma}$ , according to the relationship:

$$(e^+e^- \rightarrow e^+e^-R) = \frac{8(2J+1)}{M^3} \alpha^2 \Gamma_{R \rightarrow \gamma\gamma} f(E),$$

where  $f(E)$  is a function of the beam energy which takes into account the energy spectrum of the virtual photons. It is clear that this kind of experiments offers a very interesting tool in order to measure the quantity  $\Gamma_{R \rightarrow \gamma\gamma}$ , a parameter not easily accessible by other methods. It is however to be kept in mind that this resonance production occurs in presence of Born terms which are not negligible and which give interference effects which have to be taken into proper account. In the case of the  $\gamma\gamma \rightarrow \pi^+\pi^-$  reaction, the Born term cannot explain by itself the experimental rate, so that a possible contribution of the  $\epsilon$  meson ( $M = 660$  MeV,  $J^{PC} = 0^{++}$ ) has been assumed for the two events whose  $M_{\gamma\gamma}$  is 600 and 650 MeV respectively. With this assumption the  $\epsilon \rightarrow \gamma\gamma$  width turns out to be:

$$\Gamma_{\epsilon \rightarrow \gamma\gamma} = 10^{+12}_{-8} \text{ keV.}$$

As far as the  $\gamma\gamma \rightarrow$  many hadrons process is concerned, the event with  $M = 800 \pm 90$  MeV may be assigned either to the  $\gamma\gamma \rightarrow \eta'$  process ( $M = 958$  MeV;  $J^{PC} = 0^{-+}$ ) or to a hardly calculable non resonant contribution of  $\gamma\gamma \rightarrow$  hadrons. The resulting values for the  $\eta' \rightarrow \gamma\gamma$  with are respectively:

$$\Gamma_{\eta' \rightarrow \gamma\gamma} \begin{cases} = 11^{+15}_{-8} \text{ keV} & (\gamma\gamma \rightarrow \eta' \text{ case}) \\ = 33 \text{ keV} & (\gamma\gamma \rightarrow \text{mh non resonant}). \end{cases} \quad (95\% \text{ c. l.})$$

TABLE III.2.4  
Experimental requirements and collected data

Reaction $e^+e^-$	Wide angle detectors						Collected data			
	Tagging counters	Geometry	Penetration (iron equiv.)	Coplanarity	Colli- nearity	Prongs	nb <sup>-1</sup>	Events	$M^*$ (MeV)	Estimated contaminations (events)
$e^+e^-e^+e^-$	Both firing: $e^+e^-$ momenta measured to $\pm 5\%$	2 prongs fully devel- oping in the oppo- site tele- scopes	40 gcm <sup>-2</sup> in one telescope 10 gcm <sup>-2</sup> in the opposite tele- scope	$\Delta\varphi < 5^\circ$ (found $1^\circ, 3^\circ$ on the aver- age on 14 events)	None	Non-showering. Nuclearily inter- acting in S. C. (large angle scat- tering or trans- verse momentum unbalancing stops)	350 at an average total in- cident energy of 2.7 GeV	3	600 ( $\pi\pi$ ) 650 ( $\pi\pi$ ) 1300(?)	$\gamma\gamma \rightarrow \mu^+\mu^-$ $< 0.2$  $\gamma\gamma \rightarrow e^+e^-$ $< 0.2$
$e^+e^-$ many ( $>2$ ) hadrons	Both firing: $e^+e^-$ momenta mea- sured to $\pm 5\%$	At least 2 prongs	22 gcm <sup>-2</sup> in one telescope 10 gcm <sup>-2</sup> oppo- site telescope	None ( $\Delta\varphi > 8^\circ$ )	None	Non-showering	350 at $2E =$ $= 2.7$ GeV	2	800 1400	Negligible

\*  $M_{\gamma\gamma}$  is the  $\gamma\gamma$  invariant mass as determined by the measured energies of the forward emitted  $e^\pm$ ; the uncertainty on  $M_{\gamma\gamma}$  is  $\pm 90$  MeV.

### 3. Collinear hadrons production

#### a) Proton time-like form factor

Data have been taken [28] at ADONE with the set-up of Fig. 15 at  $E = 1.05$  GeV corresponding to proton (antiproton) kinetic energies of about 100 MeV. The differential cross section is predicted to be

$$\frac{d\sigma}{d\Omega} = \frac{\alpha^2}{8s} \beta_p \left\{ (1 + \cos^2 \theta) |G_M|^2 + \frac{4M_p^2}{s} \sin^2 \theta |G_E|^2 \right\},$$

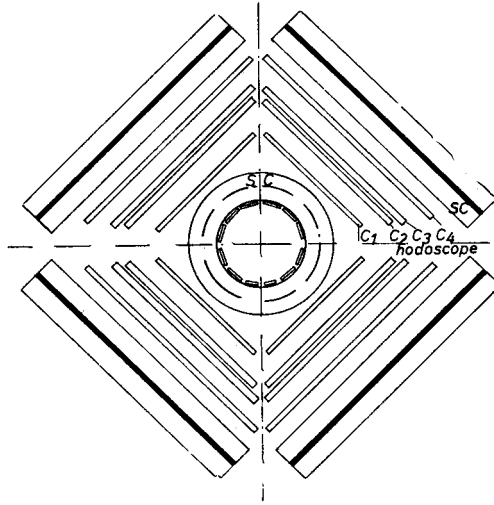


Fig. 15.  $\bar{p}p$  Naples-group apparatus (ADONE)

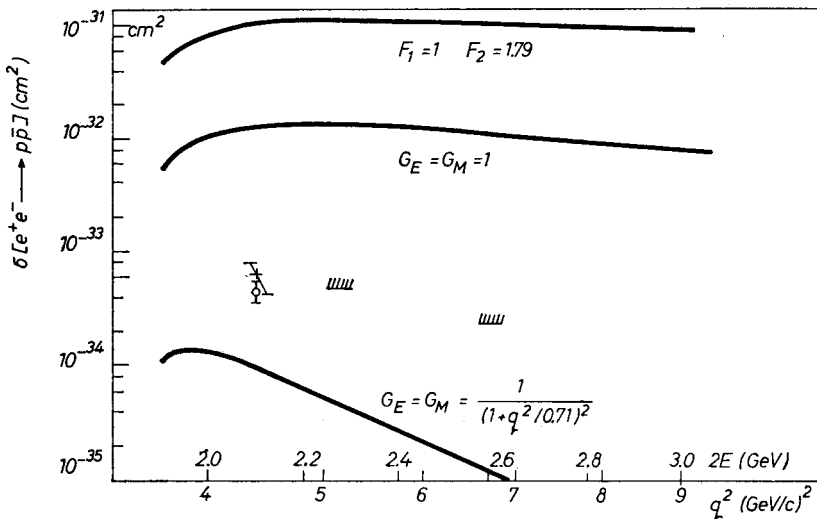


Fig. 16. Results of Naples-group on reaction  $e\bar{e} \rightarrow \bar{p}p$ :  $\bullet$  — cross section determined from all detected events,  $\times$  — cross section determined from  $\bar{p}$  star events,  $|||$  — upper limits from  $\bar{p}p \rightarrow e\bar{e}$

with  $\beta_p$  the proton velocity,  $\theta$  the proton angle with the beam line,  $G_{M,E}$  the Sachs form factors.

$G_E = G_M$  at threshold,  $s_t = 4M_p^2$ , because of kinematic singularities. Assuming that this equality holds true at  $s = 4 \times (1.05)^2 \text{ GeV}^2$

$$\frac{d\sigma}{d\Omega} \simeq \frac{\alpha^2}{4s} \beta_p |G|^2,$$

with  $G = G_E = G_M$ .

After  $25 \pm 6$  well identified pairs (range, energy loss, time of flight, collinearity and  $\bar{p}$  star used for identification), the total cross section (reported in Fig. 16) is

$$\sigma_T = (0.91 \pm 0.22) \text{ nbarn}, \quad |G| = 0.27 \pm 0.04.$$

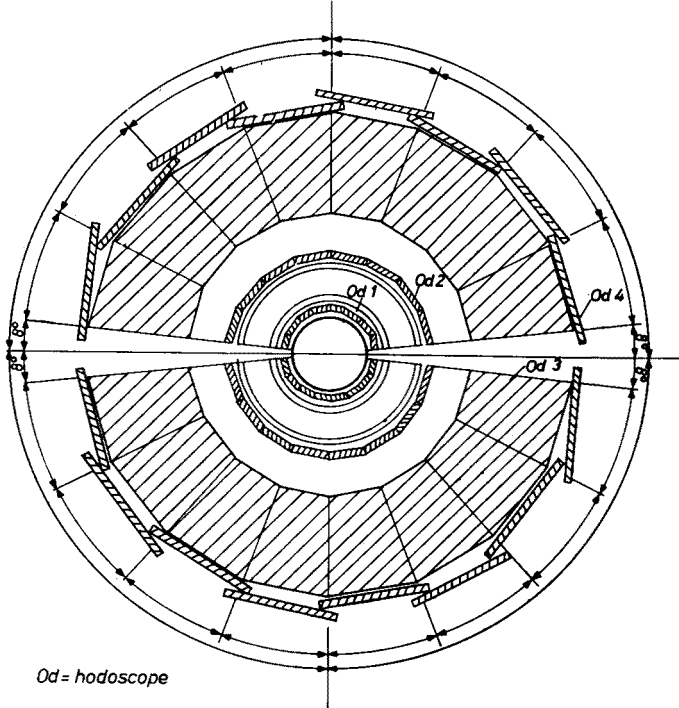


Fig. 17. BB Frascati-Pisa-Naple apparatus at ADONE

Further measurements with a new apparatus (Fig. 17) are in progress at lower energies,  $E = 1.00 \text{ GeV}$ , to check the threshold behaviour of  $|G|$ .

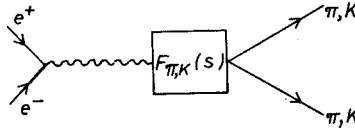
b) Meson time-like form factors

The time-like region of four-momentum transfers of the electromagnetic form factors of pions and kaons,  $F_\pi(q^2)$  and  $F_K(q^2)$  respectively, is investigated via the two-body electron positron annihilation reactions:

$$e^+e^- \rightarrow \pi^+\pi^-, \tag{1}$$

$$e^+e^- \rightarrow K^+K^-. \tag{2}$$

The one-photon approximation for these reactions leads to considering the following diagrams:



and the resulting connections among the cross sections and the form factors:

$$\frac{d\sigma}{d\Omega} = \frac{\pi\alpha^2}{4} \frac{\beta_{\pi,K}^3}{q^2} |F_{\pi,K}(q^2)|^2 \sin^2 \theta,$$

$$\sigma = \frac{\pi\alpha^2}{3} \frac{\beta_{\pi,K}^3}{q^2} |F_{\pi,K}(q^2)|^2,$$

where  $d\sigma/d\Omega(s)$  is the differential (total) cross section for the reactions (1) and (2) respectively.

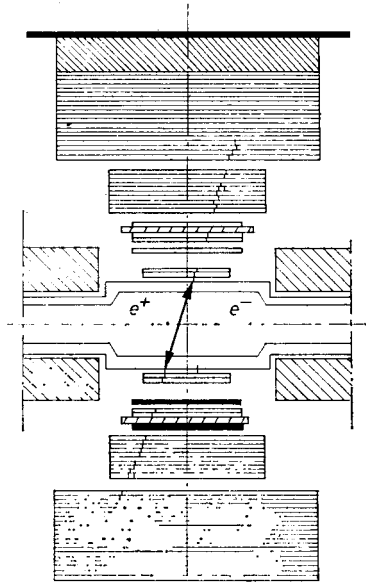


Fig. 18. NOVOSIBIRSK set-up for the  $q^0$  experiment

An extensive series of measurements of these cross sections have been performed in Novosibirsk [29–32], Orsay [33–38] and Frascati [39–42] for  $q^2$  values ranging from 0.3 to 9 (GeV/c)<sup>2</sup>. The set-ups of Novosibirsk and Orsay are shown in Figs 18, 19.

It was a success of the Vector Dominance Model: the experimental evidence that the governing process in the low  $q^2$  region ( $q^2 < 1$  (GeV/c)<sup>2</sup>) was the production of unstable vector meson  $\rho$ ,  $\omega$ ,  $\varphi$ .

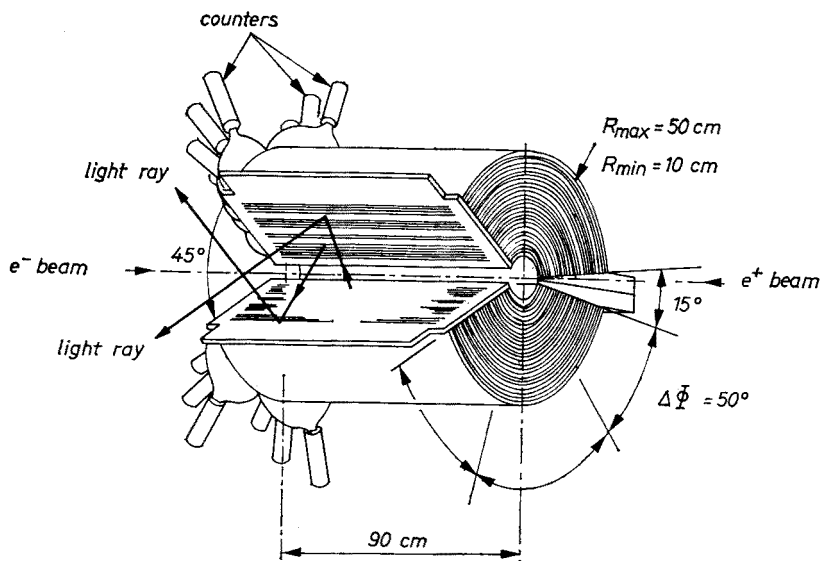
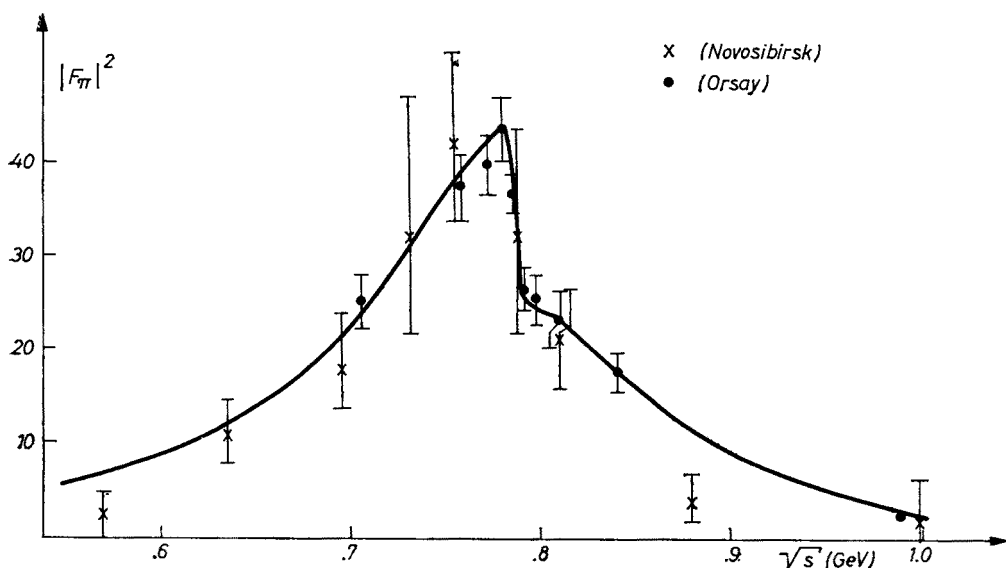


Fig. 19. ACO set-up

Fig. 20.  $|F_\pi|^2$  for  $0.5 < 2E < 1.0$  GeV

The vector mesons role with their coupling to the photon shows up very clearly in the  $q^2 < 1(\text{GeV}/c)^2$  region, where bumps in the  $e^+e^-$  annihilation cross sections have been found just at the known vector meson masses in the reaction channels accessible via the vector mesons decays.

As well known, V. D. M. has been suggested via photoproduction channels; the not unexpected production of  $\rho$ ,  $\omega$ ,  $\phi$  in the annihilation channel has allowed a thorough

analysis of the V. D. M. model. The results of this kind of measurements are shown in Figs 20, 21, 22.

From an experimental stand point it is worth recalling that relatively high values of the cross sections are reached at the energies of the peaks (for instance of the order of  $1 \mu\text{b}$  in the case of the reaction  $e^+e^- \rightarrow \pi^+\pi^-$  at  $s = M_\rho^2$ ).

When the reaction  $e^+e^- \rightarrow \pi^+\pi^-$  is considered (see Fig. 20), care must be taken [36, 38] of the distortions induced by the  $\rho-\omega$  interference effects. This kind of effects is due to the  $\omega \rightarrow \pi^+\pi^-$  transition amplitude interfering with the  $\rho \rightarrow \pi^+\pi^-$  amplitude. The  $\omega$  meson production via the  $e^+e^-$  annihilation channel is shown in Fig. 22 where the dominant  $\omega$  decay channel  $\pi^+\pi^-\pi^0$  is detected [43].

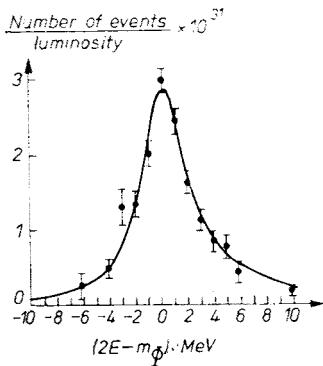


Fig. 21. Excitation curve for  $e^+e^- \rightarrow K^+K^-$   
( $2E \approx M_\phi$ )

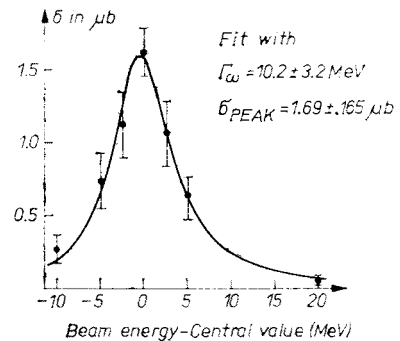


Fig. 22. Excitation curve for  $e^+e^- \rightarrow \pi^+\pi^-\pi^0$   
( $2E \approx M_\omega$ )

By introducing the  $\rho-\omega$  interference effect in a Gounaris-Sakurai [44] type of pion form factor expression a satisfactory fit to the experimental points is obtained with the following values for the parameters [38]:

$$M_\rho = (772.3 \pm 5.9) \text{ MeV}, \quad \Gamma_\rho = (135.8 \pm 15.1) \text{ MeV}, \quad \sqrt{B(\omega \rightarrow \pi^+\pi^-)} = 0.17 \pm 0.05, \\ B(\omega \rightarrow \pi^+\pi^-) = \Gamma_{(\omega \rightarrow 2\pi)} / \Gamma_{(\omega \rightarrow \text{all})}, \quad \varphi = (88.3 \pm 15.8)^\circ \text{ (relative phase of the } \rho \rightarrow \pi\pi \text{ and } \omega \rightarrow \pi\pi \text{ transition amplitudes)}, \\ B(\rho \rightarrow e^+e^-) = (4.2 \pm 0.4) \cdot 10^{-5}, \quad \Gamma_{(\rho \rightarrow e^+e^-)} = (5.8 \pm 0.5) \text{ keV}, \\ (g_\rho^2/4\pi) = 2.38 \pm 0.18, \quad (g_{\rho\pi\pi}^2/4\pi) = 2.60 \pm 0.32.$$

This Gounaris-Sakurai fit to the experimental data may be extrapolated at higher  $q^2$  values, where it represents a possible estimate of the  $\rho$  meson tail. This prediction at higher energies as well as other estimates based on modified  $\rho$  propagators with different high-energy behaviour [45] or other approaches which take into account the possible existence of higher mass  $\rho$ -like vector mesons ( $\rho'$ ,  $\rho''$ , ...) will be considered in order to interpret the high energy data as collected at ADONE (see Fig. 23).

The  $K^\pm$  electromagnetic form factor is dominated by the  $\phi$  meson production as shown in Fig. 21. The  $\phi$  production dominating mechanism has been also evidenced by measuring excitation curves of the other possible decay channels  $\phi \rightarrow K_s^0 K_L^0$  and  $\phi \rightarrow \pi^+\pi^-\pi^0$ . By analysing these experiments the following values may be assumed for the relevant

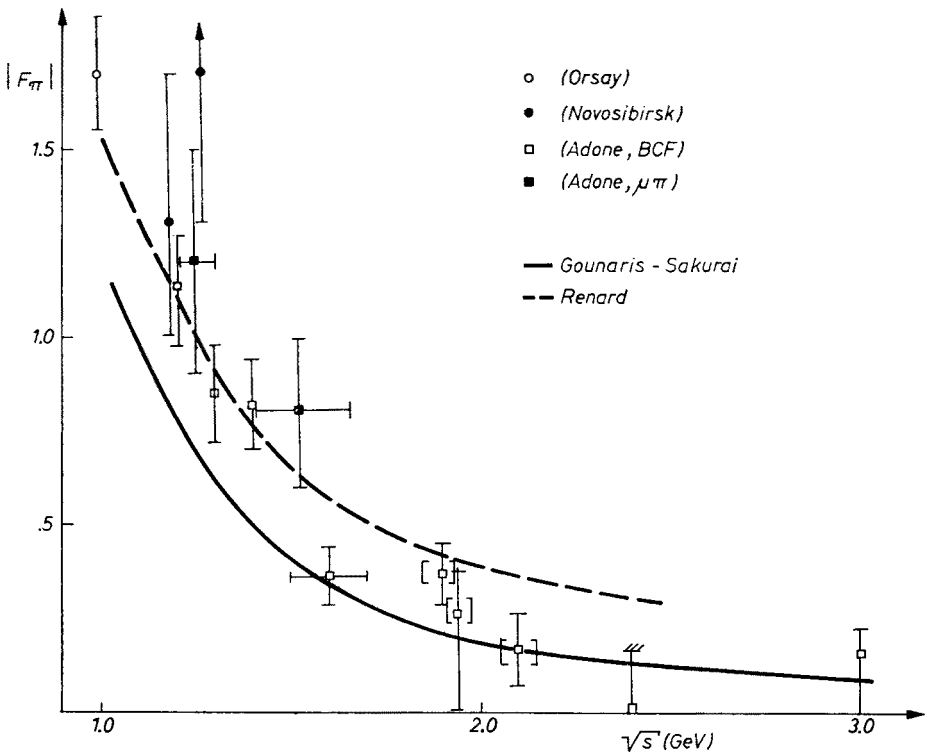


Fig. 23. Results on  $F_\pi$  for  $1.0 \leq 2E \leq 3.0$  GeV

production parameters in  $e^+e^-$  annihilation processes according to the Orsay and Novosibirsk data [46]:

The  $q^2 > 1(\text{GeV}/c)^2$  region of the meson form factors has been so far explored at Novosibirsk [32] and Frascati [39–42].

The general trend of these results is that no outstanding bump shows up and the total number of observed pairs ( $\pi^+\pi^-$  and  $K^+K^-$ ) more or less agrees with what expected by considering reasonable tails of the known vector mesons  $\rho$ ,  $\omega$ ,  $\varphi$ . All this resulted in rather low counting rates corresponding to cross sections in the range  $0.1 \div 10 \text{ nb}$  with the further experimental limitation of a  $\pi$  versus  $K$  separation possible only in a fraction of the explored  $q^2$  range.

	Orsay	Novosibirsk
$\sigma(e^+e^- \rightarrow \varphi \rightarrow \text{ll at } q^2=M^2)$	$(4.99 \pm 0.40) \cdot 10^{-30} \text{ cm}^2$	$(3.96 \pm 0.35) \cdot 10^{+30} \text{ cm}^2$
$\Gamma_\varphi$	$(4.09 \pm 0.29) \text{ MeV}$	$(4.67 \pm 0.42) \text{ MeV}$
$\Gamma_{(\varphi \rightarrow e^+e^-)}/\Gamma_{(\varphi \rightarrow \text{all})}$	$(3.52 \pm 0.28) \cdot 10^{-4}$	$(2.81 \pm 0.25) \cdot 10^{-4}$
$\Gamma_{(\varphi \rightarrow e^+e^-)}$	$(1.44 \pm 0.12) \text{ keV}$	$(1.31 \pm 0.12) \text{ keV}$



The experimental results in the region  $1 < 2E < 3$  GeV concerning the reactions  $e^+e^- \rightarrow \pi^+\pi^-$  and  $K^+K^-$  are shown in Figs 23 and 24. It turns out that with the first generation of ADONE apparata no  $\pi/K$  separation is possible above  $q^2 \simeq 3$  (GeV/c)<sup>2</sup>, so that a direct measurement of  $|F_\pi|$  and  $|F_K|$  was achieved only up to this value of  $q^2$ . In this case the experimental ratio of  $(K^+K^-)$  to  $(\pi^+\pi^-)$  pairs turns out to be of the order of one and, in agreement with the estimate [41], one can get it by using simple SU(3) and linear, zero-width, pole terms for the known vector mesons. By assuming the validity of this prediction

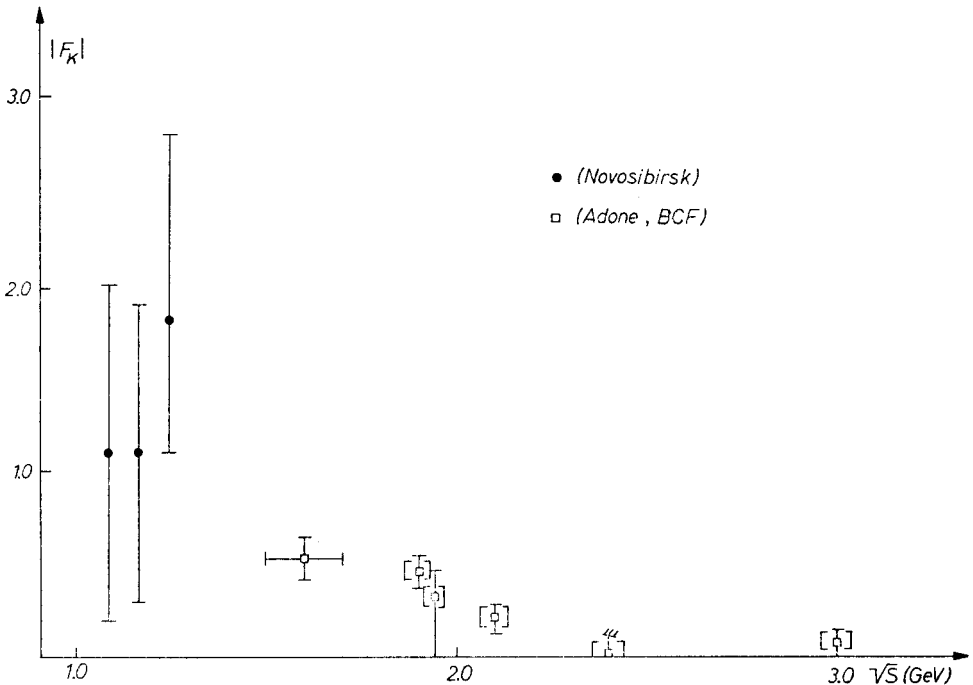


Fig. 24. Results on  $F_K$  for  $1.0 \leq 2E \leq 3.0$  GeV

for the ratio  $N(K^+K^-)/N(\pi^+\pi^-)$  in the whole  $q^2$  range explored, a separation of pions from kaons is possible and  $|F_\pi|$  and  $|F_K|$  can be determined. The resulting values of  $|F_\pi|$  and  $|F_K|$  for  $q^2 > 2.6$  (GeV/c)<sup>2</sup> obviously depend on the theoretical model and are in bracket in Figs 23 and 24.

The pion form factor in the  $q^2 > 1$  (GeV/c)<sup>2</sup> region, as shown in Fig. 23, must be obviously affected by the tails of the known vector mesons ( $\rho$ ,  $\omega$ ,  $\varphi$ ). In Fig. 23 the extrapolation of the Gounaris-Sakurai fit is also reported as a reasonable indication of the importance of the  $\rho$  tail at higher energies. Of course different estimates of the known vector mesons tails at higher energies may be done [45, 47], and this uncertainty clearly affects any possible interpretation of discrepancies between the experimental data and the predictions. For instance the  $|F_\pi|$  experimental points in the energy region  $1.2 \leq s \leq 1.4$  GeV lie systematically above the Gounaris-Sakurai prediction for the  $\rho$  tail (the number of  $(\pi^+\pi^-)$  events observed [14] in this energy range is 35, while the Gounaris-Sakurai predic-

tion amounts to 15 events). This could indicate either the existence of higher vector mesons ( $\varrho'$ ,  $\varrho''$ , ...) decaying to some extent into  $2\pi$ 's and therefore giving rise to interference effects with the known vector mesons [47], or more simply a complex structure of the  $\varrho$ ,  $\omega$ ,  $\varphi$  tails which properly includes inelastic effects of all the possible hadronic decay channels coupled to  $\varrho$ ,  $\omega$  and  $\varphi$  [45].

The present status of the knowledge does not allow one to disentangle this question.

Furthermore one could ask: what do we mean really by the expression  $F_\pi(q^2)$ ? The meaning is contained in the expression

$$\sigma_{\pi\pi} = \frac{\pi\alpha^2}{3s} \beta_\pi^3 |F_\pi(q^2)|^2,$$

but to use it directly in a theory can become rather difficult. In fact whenever  $q^2 \sim M_V^2$ ,  $M_V$  being the mass of a new vector meson, we must expect an enhancement in the total hadronic cross section. It may be in particular that also the channel  $e^+e^- \rightarrow \pi^+\pi^-$  is increased through the chain

$$\sigma_{\pi\pi} = \sigma(e^+e^- \rightarrow M_V) \frac{\Gamma_{\pi\pi}}{\Gamma_{\text{TOT}}},$$

and this can make  $\sigma_{\pi\pi}$  larger than any Gounaris-Sakurai prediction. So the very fact is that function  $\sigma_{\pi\pi}(s)$  is not easily predictable, for it depends on many uncertain parameters. One would say that  $\sigma_{\pi\pi}(s)$  is rather a mean to study, through the particular channel  $e^+e^- \rightarrow \pi^+\pi^-$ , the hadronic nature of the photon.

So, as far as the existence of higher mass vector mesons is concerned, it seems that the most adequate approach turns out to be the study of the proper exclusive channels (like  $\omega^0\pi^0$ ,  $\varrho^0\pi^0$ , etc.) at all energies.

#### 4. Multihadron production

##### a) Exclusive channels

The results on exclusive hadrons channel production must be understood with two points in mind, which are at the real basis of the  $e^+e^-$  annihilation physics.

1) The one-photon channel is very dominant respect to the other channels, in the reactions  $e^+ + e^- \rightarrow$  hadrons. This means that the quantum numbers of a final state must be those of a photon, that is  $J = 1$ ,  $P = -1$ .



The important consequence is that we know a priori the quantum numbers of any final state, and that any new particle  $M_V$  produced in an annihilation  $e^+e^- \rightarrow M_V$  must be a vector boson. In this sense, any  $e^+e^-$  storage ring is a "monochromator" not respect to the wave lengths, but in the space of Quantum Numbers.

Rarely does a hadron physicist have the luxury of such a state of well defined quantum numbers.

2) The statistics we can collect at  $e^+e^-$  storage rings are usually rather poor. This goes with the fact that the annihilation cross sections have necessarily a reduction  $\alpha^2$  in the cross sections in front of hadrons induced cross sections.

$$\frac{\sigma_{(e^+e^- \rightarrow)}}{\sigma_{(h+h \rightarrow)}} \approx 10^{-4}.$$

Therefore we measure our cross sections by the nanobarns rather than by the millibarns, as for instance in the pp (ISR) ring, while the luminosity have the same order of magnitude. These two facts may explain the success of the  $e^+e^-$  into hadrons annihilation physics as well as the difficulty in getting new results.

When more than two hadrons are produced the separation of particular channels is made difficult, especially when small solid angles are covered, by the inefficiency in the detection of low energy charged particles, and low energy  $\gamma$  rays.

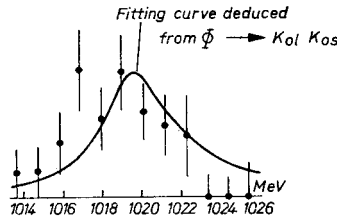


Fig. 25. Excitation curve for  $e^+e^- \rightarrow \pi^+\pi^-\pi^0$  ( $2E \approx m_\phi$ )

However, it is possible to obtain from the experimental data the number of events belonging to the simplest final configurations (3 or 4 pions in the final state) and possibly look for kinematical or geometrical features to distinguish among the various channels which can produce such configuration.

The first exclusive channel which has been investigated is

$$e^+e^- \rightarrow \pi^+\pi^-\pi^0. \quad (1)$$

This channel can be isolated by measuring the charged  $\pi$ 's momenta or by counting not more than 2 charged particles and  $2\gamma$ 's on a very large solid angle.

At Orsay energy [35] the cross section for this process is obtained by not collinear 2 prongs events and the results (Figs 22, 25) show very clearly the  $\omega$  and  $\phi$  peaks in the excitation curve.

At ADONE energies this process has been investigated by  $\gamma\gamma$ -group with the apparatus of Fig. 26. The most important experimental problem results in the separation from the background due to  $\pi^+\pi^-\pi^0\pi^0$  where only one or two  $\gamma$ 's are seen in the apparatus because of the smallness of the solid angle ( $\sim 20\%$  of  $4\pi$ ) and the relative inefficiency for low energy  $\gamma$  detection ( $E \lesssim 100$  MeV). The authors have carried out a statistical analysis of the events  $2T1\gamma$  and  $2T2\gamma$  and have given the values (of the order of a few nbarn) for the cross section in the region between  $2E = 2.0$  GeV and  $2E = 3.0$  GeV.

The second channel which can be investigated is

$$e^+e^- \rightarrow \pi^+\pi^-\pi^+\pi^-. \tag{2}$$

Also without the magnetic measure of particles momenta, the measure of the angles of the four “seen” particles gives a “OC” fit and allows the separation of the events belonging to channel [2] from the background due to channels with more than four particles produced, if this background is not too large and if *K* production is negligible.

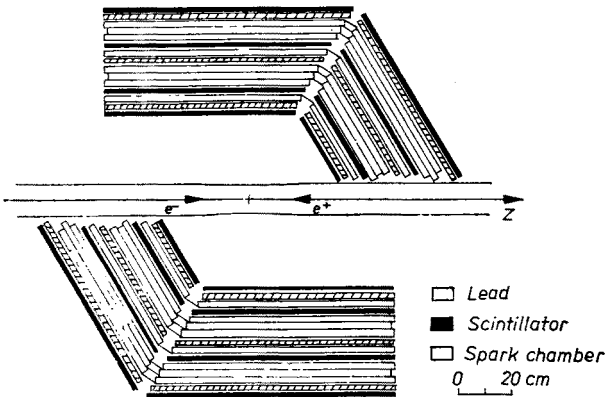


Fig. 26. Set-up  $\gamma\gamma$ -group (ADONE)

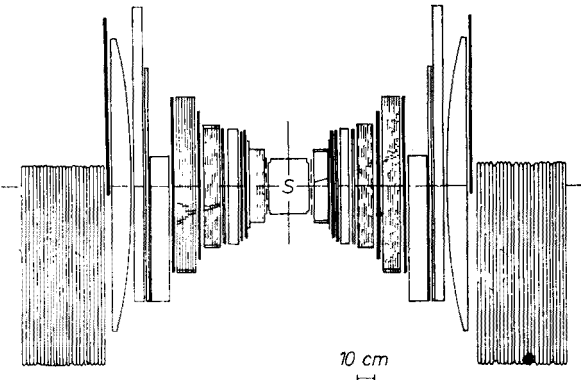


Fig. 27. Set-up of  $\mu\pi$ -group (ADONE)

This is indeed the case up to  $2E = 2 \text{ GeV}$  the experiment was carried out by the  $\mu\pi$  group at ADONE with the apparatus shown in Fig. 27. The data are reported in Table III.4.1. where the number refers to the number of 4 prongs events which fit the kinematic reconstruction corrected, via a Monte Carlo simulation of the experiment, on the basis of the 4 prongs events which do not fit the reconstruction.

It we calculate  $\sigma$  according to an I. P. S. (Independent Phase Space) distribution we obtain a broad enhancement in the value of  $\sigma$  around 1600 MeV [50], which can be related to the existence of a vector meson.

TABLE III.4.1

$2E$ (GeV)	$L$ (nb)	$4\pi$ events
1.2	5.1	0
1.3	5.8	2
1.4	11.0	6
1.5	27.0	10
1.6	40.0	12
1.65	19.5	6
1.7	40.0	11
1.9	43.5	4
2.1	163.0	6
2.4	49.7 <sup>a</sup>	1

With the events belonging to the energies from 1.4 to 1.7 GeV the following production mechanisms

- a)  $e^+e^- \rightarrow \pi^+\pi^-\pi^+\pi^-$  with the four pions produced according to I.P.S.
- b)  $e^+e^- \rightarrow \varrho^0\pi^+\pi^-$  with the  $\varrho\pi\pi$  system produced according to I.P.S.
- c)  $e^+e^- \rightarrow A_1^\pm\pi^\mp$
- d)  $e^+e^- \rightarrow \varrho^0\varepsilon^0$

have been investigated by comparing the momentum distribution of the pions with I.P.S. prediction and examining the scattering plot of  $M(\pi_1\pi_2)$  versus the invariant mass of the remaining pair (Fig. 28) and the ratio between 2-2 and 3-1 prongs into the two opposite telescopes of the set-up.

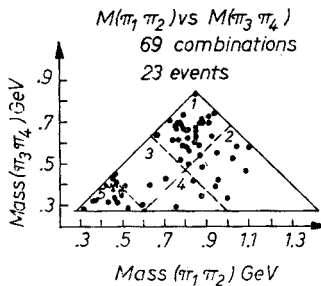


Fig. 28. Scattering plot  $M_{\pi_1\pi_2}$  vs  $M_{\pi_3\pi_4}$  ( $1.4 \text{ GeV} \leq 2E \leq 1.6 \text{ GeV}$ )

This analysis [51] leads to the conclusion that the process (2) is compatible in this energy region with 100%  $\varrho^0\varepsilon^0$  intermediate state.

A similar analysis [52] shown in Fig. 29 has been carried out for the events in the  $2E$  region  $1.9 \div 2.1 \text{ GeV}$  and suggests the hypothesis of  $\varrho^0S^*$  production so that the production mechanism appears to be the following

$$e^+e^- \rightarrow \varrho^0 + (\pi^+\pi^-)_{s\text{-wave}} \rightarrow \pi^+\pi^-\pi^+\pi^- \quad (3)$$

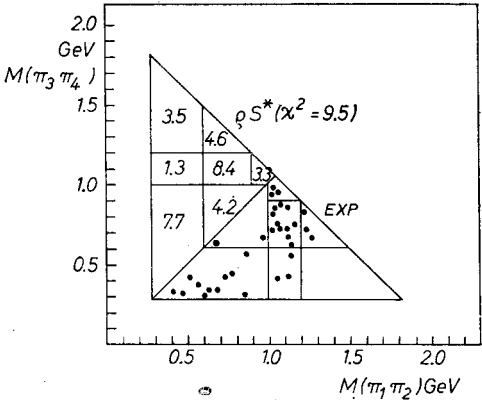


Fig. 29. Scattering plot  $M_{\pi_1\pi_2}$  vs  $M_{\pi_3\pi_4}$  ( $1.9 \text{ GeV} \ll 2E \ll 2.1 \text{ GeV}$ )

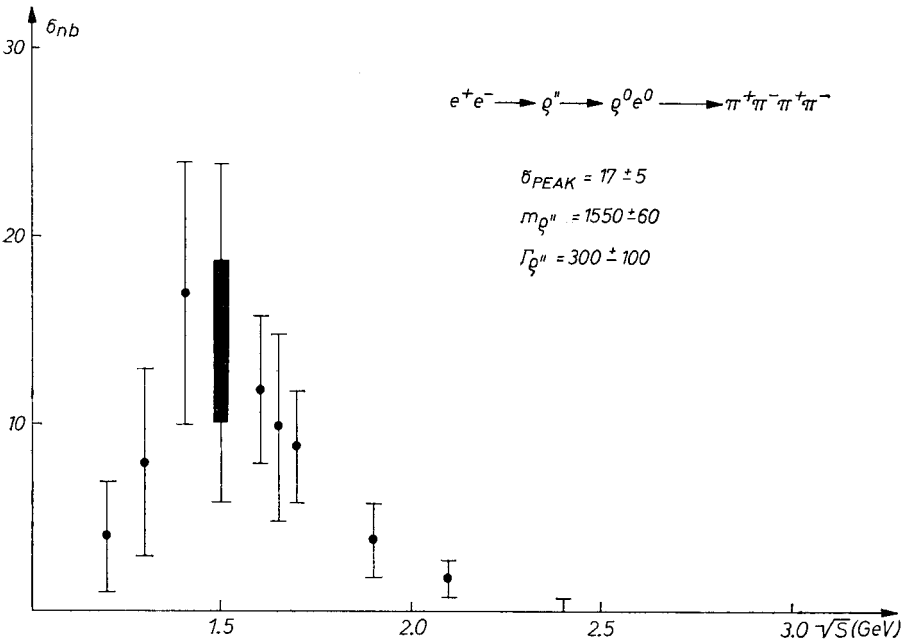


Fig. 30. Excitation curve for  $e^+e^- \rightarrow \rho^0 \rightarrow \rho^0(\pi\pi)_{s\text{-wave}}$

Under this hypothesis and utilizing also all the events with 3 or 4 prongs seen into the set-up we obtain for the cross section of the process (3) the values reported in Table III.4.2 and in Fig. 30.

TABLE III.4.2

1.2	1.3	1.4	1.5	1.6	1.65	1.7	1.9	2.1	2.4
$4 \pm 3$	$8 \pm 5$	$17 \pm 7$	$15 \pm 4 \pm 5$	$12 \pm 4$	$10 \pm 5$	$9 \pm 3$	$4 \pm 2$	$2 \pm 1$	1

The result of a Breit-Wigner fit of these data gives

$$\sigma_{\text{peak}} = 17 \pm 5 \text{ nbarn}, \quad M_{\rho''} = 1550 \pm 60 \text{ MeV}, \quad \Gamma_{\rho''} = 300 \pm 100 \text{ MeV}.$$

In order to obtain the  $\rho''$  coupling constant one must assume the value for the ratio  $r$

$$r = \frac{\rho'' \rightarrow \pi^+ \pi^- \pi^+ \pi^-}{\rho'' \rightarrow \pi^+ \pi^- \pi^0 \pi^0}.$$

Assuming  $r = 2$  (i. e.  $\rho''$  decays only through  $\rho^0 \epsilon^0$ ) we obtain

$$f_{\rho''}^2/4\pi = 18 \pm 5$$

(for  $r = 1$  we should have obtained for this value  $13 \pm 4$ ).

The interpretation of this enhancement as a vector meson has been extensively questioned in the last year.

Our present knowledge about the  $\rho''$  is summarized in the following table (v. Moffeit, report to the 1973 Bonn Conference) [53].

Reaction	$J^P$	$I^G$	$M$ (MeV)	$\Gamma$ (MeV)	$\Gamma_{(\rho'' \rightarrow \pi^+ \pi^-)}/\Gamma_{(\rho'' \rightarrow \text{all})}$
$e^+e^- \rightarrow \rho^0 \pi^+ \pi^-$	$1^-$	$1^+$	1550	300	—
$\gamma p \rightarrow \rho^0 \pi^+ \pi^- p$ ( $\gamma$ pol)	$1^-$	$1^+$	1500	600	$< 0.2$
$\pi^- p \rightarrow \pi^+ \pi^- n$ (phase shift analysis)	1	1	$1590 \pm 20$	$180 \pm 50$	$= .25 \pm .02$

The channel (2) has been measured at high energies at SPEAR. In this case the events were identified by measuring all the angles and momenta (4C Fit). The small value of the cross section at this energies supports the arguments in favour of the resonance interpretation and against other interpretation as  $\rho$  form factor modification, or Deck effect.

The channel

$$e^+e^- \rightarrow \pi^+ \pi^- \pi^0 \pi^0 \tag{4}$$

has been clearly measured by Orsay [54] group in an experiment where the events belonging to this channel were identified by counting at least  $1\pi^\pm, 3\gamma$ 's in a large solid angle apparatus.

The result (Fig. 31) shows a very clear threshold effect for  $\pi^+ \pi^- \pi^0 \pi^0$  production via two body  $\omega_0 \pi^0$  production.

At ADONE [55] the  $\mu\pi$  group measured only charged particles, but it was possible to evaluate the events belonging to final states with only 2 charged particles between the 2-prongs not coplanar events. This task was achieved by subtracting the background due to channel with at least 4 charged particles in a fairly model-independent way, based on the circumstance that for these events the ratio between the probability of seeing 2 prongs and 3 or 4 prongs in the set-up is almost independent from the particular channel.

If one takes into account the fact that  $\pi^+\pi^-\pi^0$  ( $\gamma\gamma$  group result) and  $\pi^+\pi^-\pi^0\pi^0\pi^0$  ( $\sigma_{\pi^+\pi^-\pi^0\pi^0} = \frac{1}{2} \sigma_{\pi^+\pi^-\pi^+\pi^-\pi^0}$  [56] which is small up to 1.5 GeV,  $\mu\pi$  result) give a negligible contribution, these events can be assigned to the channel (4).

After subtracting the contribution of  $\rho''$  (1600) calculated from the  $\pi^+\pi^-\pi^+\pi^-$  excitation curve the authors could obtain, by calculating efficiency according to a Monte Carlo I.P.S. simulation of the experiment, the excitation curve shown in Fig. 32 where are also reported the ACO lower energy results.

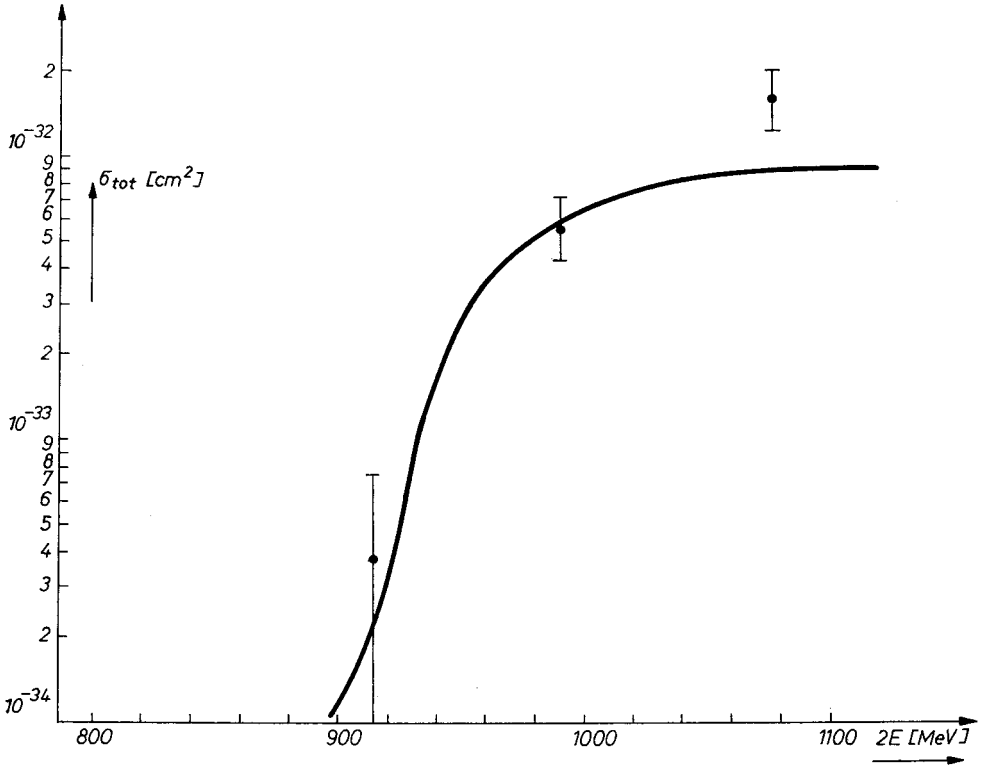


Fig. 31. ACO results on  $e^+e^- \rightarrow \pi^+\pi^-\pi^0\pi^0$

The cross section is seen to rise rapidly with increasing the total energy  $2E$  from 1.0 to 1.2 GeV reaching the value of  $\sigma \sim 70$  nb at this latter energy value.

The authors tested explicitly to which extent this result depends on the I.P.S. assumption. Assuming for instance  $\omega_0\pi^0$  or  $\rho \pm (\pi\pi)^\mp$  with  $\pi\pi$  in p-wave they found that the cross sections were essentially unchanged, within the errors for  $2E \leq 1.3$  GeV.

On the other hand, for  $2E > 1.3$  GeV the results are critically dependent on the assumed mechanism and for  $2E > 1.5$  GeV some of the hypotheses utilized to obtain the correct sample of events to work out cannot be still justified. The fast rise in the cross section between 1.0 and 1.2 GeV can hardly be interpreted as a threshold effect. As a matter of fact a similar effect if due to intermediate state as  $A_1\pi$ ,  $\rho^0\varepsilon^0$  should have, but has not been



observed in the same energy interval in  $\pi^+\pi^-\pi^+\pi^-$  excitation curve. On the other hand the threshold effect due to  $\omega_0\pi^0$  seems to be largely unable in the current theoretical scheme [57] to account for the large values of  $\sigma$  found for  $2E = 1.2, 1.3$  GeV. Thus a possible and "simple" interpretation of these results can be given in terms of a resonant state with a mass in the range  $1.2 \div 1.3$  GeV and dominant decay mode  $\varrho'(1250) \rightarrow \omega_0\pi^0$ . We examine now this possible interpretation, notwithstanding we know the limits of our evidence. Such a resonance could be responsible:

1) for the enhancement recently found at 1.24 GeV in the mass spectrum of the  $(\pi^+\pi^-\pi^0)$  system peripherally produced in high energy interaction [58];

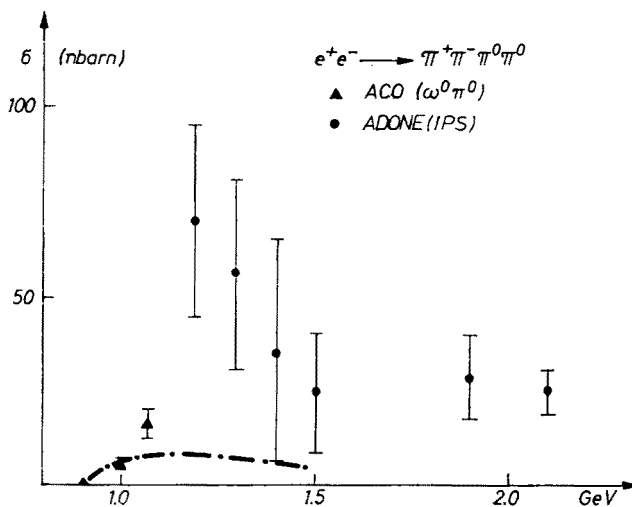


Fig. 32.  $\mu\pi$ -group results on  $e^+e^- \rightarrow \pi^+\pi^-\pi^0\pi^0$

2) for the signal observed at a mass of  $\sim 1.25$  GeV for the  $\omega_0\pi^0$  system produced by  $\bar{p}p$  annihilation [59];

3) for the indication of an excess of events in the 1.2 to 1.4 GeV region for  $\pi\pi$  production in  $e^+e^-$  interaction by ADONE groups [60], as mentioned when we treated the electromagnetic  $\pi$  form factor, and pointed out by Bramon [61].

A best fit of data based only on the values of  $\sigma$  for  $E \leq 1.3$  GeV (ACO and  $\mu\pi$ ) and assuming contributions only from  $\varrho^0$  and  $\varrho'$  ( $M = 1.25$  GeV,  $\Gamma = 150$  MeV) yields the following results

$$\sigma_{\text{PEAK}}(\omega_0\pi^0) = 120 \pm 40 \text{ nb}, f_{\varrho'}^2/4\pi = 7 \pm 2,$$

$$\varphi = 1.2 \pm 0.2 \text{ for the relative phase between } \varrho^0 \text{ and } \varrho'.$$

With the well established value of the  $\varrho$  meson coupling constant and the numerical values given for  $\varrho'$  (1250) and  $\varrho''$  (1550) coupling constants the ratios  $f^2/4m^2$  are found to be  $4.4 \pm 0.4$ ;  $4.5 \pm 1.3$ ;  $7 \pm 2$  for  $\varrho$ ,  $\varrho'$ ,  $\varrho''$  respectively.

These ratios agree with each other within the errors, fulfilling an asymptotic rule suggested in the "Extended Vector Meson Dominance model" of Bramon et al. [62].

New measurements on all these exclusive channels in the energy range  $2E = 1.15$  to  $3.0$  GeV will soon be possible at ADONE, with the “second generation” apparatus all characterized by detecting solid angles considerably larger than the ones employed in the first generation set up, with good efficiency for  $\gamma$  ray counting, or by measuring the momentum of the detected charged particles.

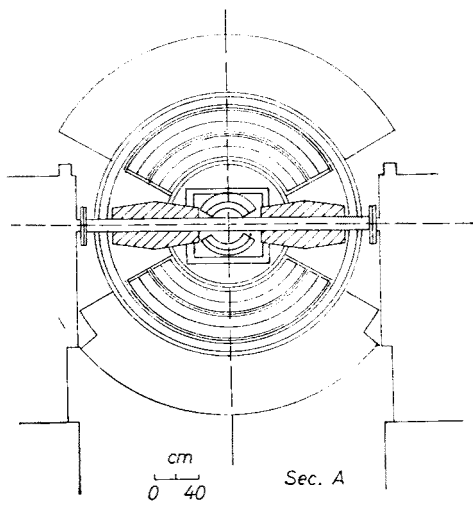


Fig. 33. MEA-group set-up (ADONE)

The MEA apparatus which is now running at ADONE is shown in Fig. 33. In the next six months this group has the program to cover the region between  $2E = 1.2$  and  $2.0$  GeV, collecting data at each  $50$  MeV energy with a statistic of about  $50$  events for each channel near the peaks.

b)  $\sigma_{TOT}$

The high values of the total cross section  $\sigma_{TOT}$  of the processes

$$e^+e^- \rightarrow \text{at least 3 hadrons}$$

is the important and unexpected discovery of the  $e^+e^-$  colliding beams.

In our case the reference cross section respect to which  $\sigma_{TOT}$  may be compared is the cross section

$$\sigma_{2 \text{ P.L.fermions}} \simeq \sigma_{\mu\mu} = \frac{4\pi}{3} \frac{\alpha^2}{s},$$

so we can say that the discovery with ADONE and with the more recent machines is the fact that in general  $\sigma_{TOT} > \sigma_{\mu\mu}$  and the ratio  $R = \sigma_{TOT}/\sigma_{\mu\mu}$  seems to increase at high energies. For what concerns the ADONE results, it has to be remembered that the first-generation set-ups were not properly designed to face the unexpected abundant production of many body final states. In particular, the rather small solid angle covered ( $\Delta\Omega/4\pi \sim 20\%$ , typi-

cally) made detectable only a limited fraction of the production particles and the lack of knowledge of the momenta of the detected particles (no magnetic analysis available) did not allow a proper estimate of what was missing of the reaction products. Thus, in order to estimate the production cross section from the rough data a certain number of assumptions had to be made, all this resulting in somewhat model-dependent analysis. In spite of these difficulties total cross section could be obtained with some confidence because the value of  $\sigma_{TOT}$  is not critically dependent on the distribution hypothesis. I now will give some detail on the analysis to understand that point.

## 5. Results from $\mu\pi$ group [63]

The  $\mu-\pi$  group evaluation of  $\sigma_{TOT}$  is based on the separation of the recorded events on the basis of the configuration seen in the apparatus (only charged particles detected).

- 1)  $2T$  events: (2 non-collinear prongs in opposite telescopes with  $\Delta\varphi > 10^\circ$ );
- 2)  $nT$  events ( $n = 3, 4, 5, 6$ ):  $n$  convergent prongs with at least one prong in each telescope.

As discussed when I talked about exclusive channels, because only an even number of charged particles (2, 4, 6, ...) can be produced, and based on the circumstance that, if we assume  $K$  production negligible, the ratios between the efficiency for seeing a given channel in the different configuration  $2T$ , 3 or  $4T$ , 5 or  $6T$  are dependent only by the number of charged and only a little by the number of  $\pi^0$ , we can obtain from the numbers of the events in these configuration the number of events belonging to channels with respectively:

$2N$ , only 2 charged  $\pi$ 's and at least one  $\pi^0$ ;

$4N$ , 4 charged  $\pi$ 's with any number of  $\pi^0$ 's; a subset of these events is the number of events with 4 prongs belonging to the channel  $\pi^+\pi^-\pi^+\pi^-$ ;

$6N$ , 6 charged  $\pi$ 's with any number of  $\pi^0$ 's.

Now we can obtain the total cross sections after making the following assumptions:

1) For the channels with only 2 charged pions we calculate the value of  $\sigma_{TOT}$  as discussed for this exclusive channel.

2) We calculate from 4 events the  $\pi^+\pi^-\pi^+\pi^-$  cross section and subtract from  $4N$  events the contribution of this channel as discussed for this exclusive channel.

3) For channels with more than  $4\pi$ 's

a) we assume invariant phase space (I.P.S.) momentum distribution for the product particles;

b) we neglect channels with  $n_{\pi^0} \geq n_{\pi^+} + n_{\pi^-}$ ;  $n_{TOT} \geq 8$ ;

c) we weight the efficiencies of the channels with the same number of charged  $\pi$ 's and different number of  $\pi^0$ 's by two extreme hypothesis,

I) the cross section of channels with an odd number of pions is negligible in front of that of channels with an even number of pions;

II) the cross section of channels with the same number of charged particles and different number of  $\pi^0$ 's are in the same ratio as for  $\bar{p}p$  annihilation at rest. In this case we also take into account the relation which results from isotopic spin rules for channels with an equal odd total number of pions;

and assume for  $\sigma_{>4}$ ,  $\sigma_6$  the mean value between the ones obtained in the hypothesis I and II with a systematic error which takes into account the difference.

Our  $\sigma_{\text{TOT}}$  is now defined as

$$\sigma_{\text{TOT}} = \sigma_2 + \sigma_4 + \sigma_{>4} + \sigma_6,$$

where also a systematic error on  $\sigma_2$  is assigned to take into account the possible existence of the  $\rho' \rightarrow \omega_0 \pi^0$ .

It must be also said that these values of  $\sigma_{\text{TOT}}$  do not take into account the existence of possible channels (as for example  $\omega_0 \pi^0$  above 1.4 GeV) that for kinematical reasons produce preferentially charged pions only in one telescope, because in this case, due to the request of seeing at least one prong in each telescope, the efficiency of the set-up is so small that no significant value can be obtained.

To assume the contribution of this channels negligible is in some extent justified by the results of  $\gamma\gamma$ -group which has not such a bias in the trigger.

### *Results from the $\gamma\gamma$ -group [64]*

The apparatus of the  $\gamma\gamma$ -group is rather different from the " $\mu\pi$ " in the triggering and in the explored  $\theta$  region. Beyond this it had a high efficiency in the detection of  $\gamma$  rays. This makes this apparatus rather orthogonal to the  $\mu\pi$  apparatus in many aspects. I feel therefore that, as the results on  $\sigma_{\text{TOT}}$  agree with each other within the errors, to average the values could be a possible and reasonable thing to do.

In order to obtain  $\sigma_{\text{TOT}}$  the  $\gamma\gamma$ -group has assumed that the most important processes which contribute to  $e^+e^- \rightarrow$  multihadrons are

- a)  $e^+e^- \rightarrow \pi^+\pi^- + n\pi^0 \quad (1 < n \leq 6),$
- b)  $e^+e^- \rightarrow m\pi^+ + m\pi^- + n\pi^0 \quad (m = 4, 6, 8; m+n \leq 8).$

The  $\sigma_{\text{TOT}}$  was found by solving the system

$$N_c = L \sum \sigma_i \varepsilon_{ic},$$

where  $L$  is the total integrated luminosity,  $N_c$  the number of events detected in a certain configuration (for instance, 1 charged + 2 photons, 2 charged + 1 photon, 3 charged, 2 charged + 1 photon...) and  $\varepsilon_{ic}$  is the efficiency to detect in a configuration  $c$  an event from the  $i$ -th channel whose partial cross section is  $\sigma_i$ .

Due to the rather poor statistics collected, the "optimal solutions" (it is required that all  $\sigma_i$  be positive) are such that the partial cross sections are not well determined, whereas the total cross section is much more reliable.

### *Other data at ADONE*

Data from Boson groups [65] suffer more from the severe limitation on the experimental set-up (not more than one particle, charged or neutral, was detected for each telescope, and only the  $\varphi$  coordinate was measured for charged particles).

Only one configuration of events (2 non-collinear charged prongs with acoplanarity angle  $> 20^\circ$ ) has a real statistical significance, while other two configurations (3 convergent

charged particles and 2 convergent charged particles + one photon) have very small detection efficiency.

This results in a larger model-dependence. Nevertheless, with the same method which has been described for the  $\gamma\gamma$ -group results, the authors succeeded to give, with large systematic errors, the results on  $\sigma_{TOT}$  — the less model-dependent quantity. These results were the first experimental proof that multihadrons production is very abundant in this energy region, a not expected situation, as I already said.

As these data within their large errors agree with the other Frascati data and because of this larger model dependence, I have not included them in the picture of the existing

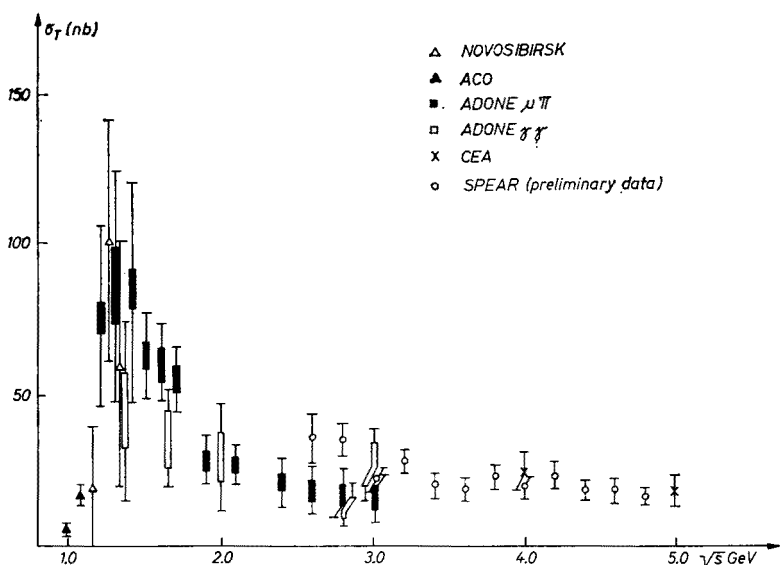


Fig. 34.  $\sigma_{hadrons, total}$  vs  $E$

data on  $\sigma_{TOT}$ , (Fig. 34), where also the results obtained at higher energies by CEA by-pass [37], and preliminary data from SPEAR are reported [38].

I must also add that results on multihadrons cross sections from BCF experiment have been presented to several conferences. This group analyses its data by assuming the same multiplicity as in  $p\bar{p}$  at rest; this assumption could be somewhat uncertain at low energies (1.2 ÷ 1.8 GeV) when resonances were present. I do not know their last data, the analysis of which is in progress and that are now close to publication.

In Fig. 35 it is shown as a function of energy the ratio  $R$  between  $\sigma_{TOT}$  (the cross section for producing a final state having at least 2 charged pions plus something else) and the cross section for producing a pair of massless ideal Dirac particles, generally called  $\sigma_{\mu\mu}$ . This ratio is useful, first because it removes some expected kinematical factors and second it emphasizes the magnitude of the cross section: we note the dramatic difference of character from the  $s$  dependence of the pion form factor squared  $\simeq 4\sigma_{\pi\pi}/\sigma_{\mu\mu}$ . The ratio  $\sigma_{TOT}/\sigma_{\mu\mu}$  is increasing with  $s$  reaching at  $s = 25$  (GeV)<sup>2</sup> a value of the order of 6.

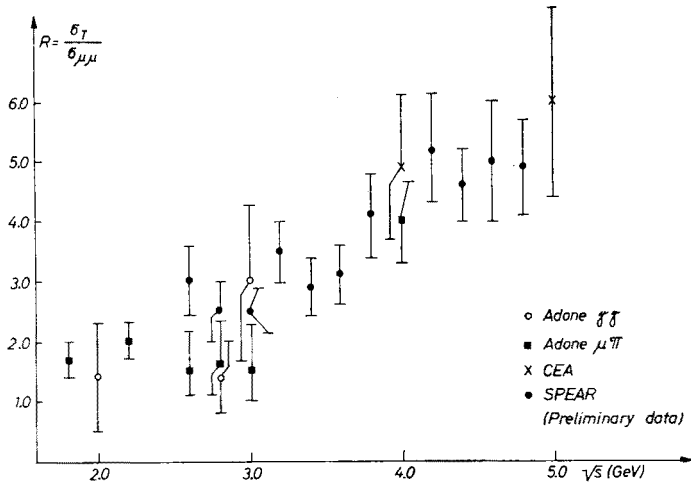


Fig. 35.  $R = \sigma_{\text{hadrons, total}} / \sigma_{\mu\bar{\mu}}$  vs  $E$

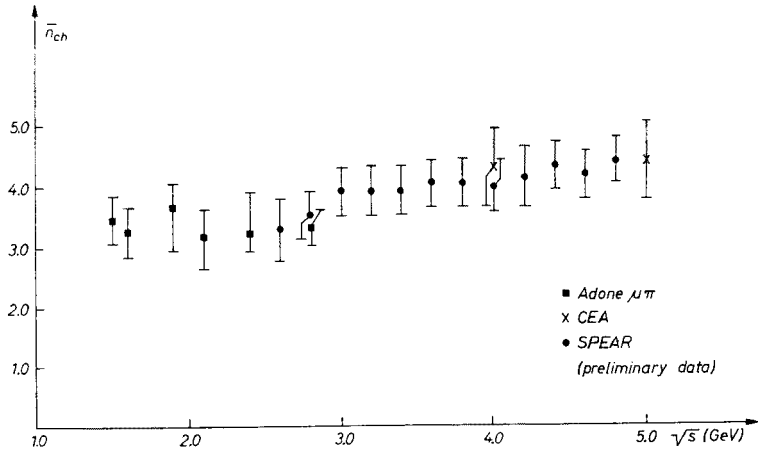


Fig. 36. Charged particles multiplicity  $\langle n_{ch} \rangle$  vs  $E$

Such a large value for  $R$  gives much trouble to quark model builders, who say that  $R_\infty = \sigma_{\text{TOT}}/\sigma_{\mu\mu} = \sum Q_i^2$  where  $Q_i$  are the charges of constituents.

The idea is that a pair of quarks are produced and they dress themselves as multi-hadrons. The model is simple and thus appealing. Unfortunately “old fashioned” quarks model predicts  $R_\infty = 2/3$  which lies far below the data. The suggestion of introducing three different kinds of quarks having colors allows one to obtain  $R_\infty = 2$ . This can work for ADONE data but is inconsistent with CEA and preliminary data from SPEAR. There are other variations which allows  $R_\infty = 10/3$ ,  $R_\infty = 4$  and also  $R_\infty = 6$ ; indeed, we have no compelling reason to believe that we have reached the asymptotic region; there is,

for example, no prohibition against the ratio peaking and then falling; in fact if one looks only at the data below  $q = 9 \text{ GeV}^2$  this is a consistent statement because of large contribution of what we call  $q'$  and  $q''$ . In the last year a considerable effort was made by theorists to give a consistent explication of SPEAR data and there are more than a model which claimed to be satisfied. The next year data at higher energies, first from SPEAR II, will aid to resolve this question. Also of interest is the observed charged multiplicity shown in Fig. 36. A simple statistical model would lead one to expect  $\langle n \rangle \sim \sqrt{s}/\langle E_\pi \rangle$ . Other models would predict a logarithmic increase similar to that observed in ordinary hadronic reactions. The existing data do not clearly distinguish between the two alternatives if an arbitrary additive constant is added.

#### REFERENCES

- [1] C. Bernardini, G. F. Corazza, G. Ghigo, B. Tombesi, *Nuovo Cimento* **18**, 1293 (1960).
- [2] C. Bernardini, G. F. Corazza, G. Di Giugno, J. Haissiusky, P. Marin, R. Querzoli, B. Tombesi, *Nuovo Cimento* **34**, 1473 (1964).
- [3] Orsay Storage Ring Group *Proc. Int. Conf. on High Energy Accelerators*, Dubna 1963, p. 288.
- [4] G. I. Budkin, *Sov. Phys. Usp.* **9**, 534 (1967).
- [5] V. L. Auslander et al., *Sov. J. Nucl. Phys.* **9**, 114 (1969); J. E. Augustin et al., *Phys. Lett.* **28B**, 508 (1969).
- [6] C. Bernardini, *Proc. Int. Symp. on High Energy*, Cornell 1971.
- [7] K. Strauch, *Proc. Int. Symp. on Electrons and Photons Interactions at High Energies*, Bonn (1973).
- [8] V. N. Baier, XLVI Varenna Course A.C.C. PRESS.
- [9] V. E. Balakin et al., *Phys. Lett.* **34B**, 99 (1971).
- [10] C. Bacci et al., *Lett. Nuovo Cimento* **2**, 73 (1971).
- [11] G. Hanson et al., *Lett. Nuovo Cimento*.
- [12] B. L. Baron et al., Bonn Int. Symp. on Electrons and Photon Interactions.
- [13] Preliminary Data from SPEAR Group, Washington 1974 Conference.
- [14] J. E. Augustin et al., *Phys. Rev. Lett.* **30**, 462 (1973).
- [15] M. Bernardini et al., Bonn Int. Symp. on Electron and Photon Interactions.
- [16] S. Orito et al., *Phys. Lett.* **48B**, 165 (1974).
- [17] For an exhaustive theoretical literature on the subject see: S. J. Brodsky, *Proc. Batavia Conf. 1972*; N. A. Romero, A. Jacarrini, P. Kessler, *CR Acad. Sci. Paris* **269B**, 153 (1969); S. J. Brodsky, T. Kinoshita, H. Terazawa, *Phys. Lett.* **25**, 972 (1970); A. Terazawa, *Rev. Mod. Phys.*
- [18] C. Bacci et al., *Proc. of the Intern. Conf. on Meson Resonances and Related Electromagnetic Phenomena*, Bologna, 1971.
- [19] G. Barbiellini, S. Orito, *Frascati Report LNF 71/17* (1971).
- [20] C. Bacci et al., *Lett. Nuovo Cimento* **3**, 709 (1971).
- [21] G. Barbiellini et al., *Frascati Report LNF 73/63* (1973); submitted to *Phys. Rev. Lett.*
- [22] V. E. Balakin et al., *Phys. Lett.* **3B**, 328-663 (1971).
- [23] C. Bacci et al., *Frascati Report LNF 73/50* (1973).
- [24] F. Ceradini et al., *J. Phys. (France)* **C2**, Suppl., 35, C2-9 (1974); G. Salvini, *J. Phys. (France)* **C2**, Supl. 35, C2-1 (1974).
- [25] S. Orito, M. L. Ferrer, L. Paoluzi, R. Santonico, *Phys. Lett.* **48B**, 380 (1974).
- [26] G. Barbiellini et al., *Frascati Report LNF 74/10 (P)* (1974); submitted to *Lett. Nuovo Cimento*.
- [27] C. Carimalo, P. Kessler, J. Parisi, *PAM* 72-12 (1972).
- [28] G. Di Giugno et al., *Nuovo Cimento* **14**, 1 (1973).
- [29] V. L. Auslander et al., *Phys. Lett.* **25B**, 433 (1967).

- [30] V. L. Auslander et al., *Sov. J. Nucl. Phys.* **9**, 144 (1969).
- [31] V. E. Balakin et al., *Phys. Lett.* **34B**, 328 (1971).
- [32] V. E. Balakin et al., *Phys. Lett.* **41B**, 205 (1972).
- [33] J. E. Augustin et al., *Phys. Rev. Lett.* **20**, 126 (1968).
- [34] J. E. Augustin et al., *Phys. Lett.* **28B**, 508 (1969).
- [35] J. E. Augustin et al., *Phys. Lett.* **28B**, 517 (1969).
- [36] J. E. Augustin et al., *Lett. Nuovo Cimento* **II**, 214 (1969).
- [37] J. C. Bizot et al., *Phys. Lett.* **32B**, 416 (1970).
- [38] D. Benaksas et al., *Phys. Lett.* **39B**, 289 (1972).
- [39] V. Alles Borelli et al., *Phys. Lett.* **40B**, 433 (1972).
- [40] M. Bernardini et al., *Phys. Lett.* **44B**, 393 (1973).
- [41] M. Bernardini et al., *Phys. Lett.* **46B**, 261 (1973).
- [42] G. Barbiellini et al., *Lett. Nuovo Cimento* **6**, 557 (1973).
- [43] J. E. Augustin et al., *Phys. Lett.* **28B**, 513 (1969).
- [44] G. J. Gounaris, J. J. Sakurai, *Phys. Rev. Lett.* **21**, 244 (1968).
- [45] F. M. Renard, *Preprint PM/73/3*, Montpellier, France.
- [46] For a review survey of the electromagnetic form factors of the hadrons see: B. Bartoli, F. Felicetti, V. Silvestrini, *Riv. Nuovo Cimento* **2**, 241 (1972).
- [47] G. Bonneau, F. Martin, *Nuovo Cimento* **13A**, 413 (1973).
- [48] A. Bramon, *Frascati Report LNF 73/40* (1973).
- [49] C. Bacci et al., *Phys. Lett.* **38B**, 551 (1972); *Phys. Lett.* **44B**, 533 (1973).
- [50] G. Barbarino et al., *Lett. Nuovo Cimento* **3**, 689 (1972).
- [51] F. Ceradini et al., *Phys. Lett.* **43B**, 341 (1973).
- [52] R. Bernabei et al., LNF 74/12 (1974) submitted to *Phys. Lett.*
- [53] Moffeit, *Report*, Bonn Conference (1973).
- [54] G. Cosme et al., *Report*, Bonn Conference (1973).
- [55] M. Conversi et al., submitted to *Phys. Lett.*
- [56] C. A. Llewellyn Smith, A. Pus, *Report Loo 35021*.
- [57] F. Renard, *Nuovo Cimento* **64A**, 979 (1969).
- [58] J. Ballam et al., SLAC PUB — 1364 (1974); submitted to *Nucl. Phys.*
- [59] P. Frenkiel et al., *Nucl. Phys.* **47B**, 61, (1972).
- [60] M. Bernardini et al., *Phys. Lett.* **46B**, 261 (1973).
- [61] A. Bramon, *Lett. Nuovo Cimento* **8**, 569 (1973).
- [62] A. Bramon, E. Etim Etim, M. Greco, *Phys. Lett.* **41B**, 609 (1972).
- [63] M. Grilli et al., *Nuovo Cimento* **13A**, 593 (1973); F. Ceradini et al., *Phys. Lett.* **47B**, 80 (1973).
- [64] C. Bacci et al., *Phys. Lett.* **38B**, 571 (1972); *Phys. Lett.* **44B**, 533 (1973).
- [65] B. Bartoli et al., *Phys. Rev.* **6D**, 2374 (1972).
- [66] A. Litke et al., *Phys. Rev. Lett.* **30**, 1189 (1973); S. Tornopolsky et al., *Phys. Rev. Lett.* **32**, 432 (1974).
- [67] Spear Magnet preliminary data, Washington Conference 1974.